Analysis of leukocytes profile

Peripheral blood was collected from heart and EDTA-2K was added. Leukocyte profiles were analyzed by use of automation instruments (Mitsubishi BCL Corp., Tokyo, Japan).

Flow cytometric analysis

Peripheral blood was collected from heart and EDTA-2K was added. After lysis for 5 min at 4 °C, subsequent centrifugation (1000×g at 4 °C, cells) was suspended in HBSS. Bone marrow cells were prepared from a shinbone. The cells were incubated with mAb against surface markers (BD Pharmingen, CA, USA). Gr-1 (RB6-8C5), Mac-1 (M1/70) were used for flow cytometric analysis, and then analyzed with FACSCalibur using CellQuest software (BD Biosciences, CA, USA).

Neutrophil function assay

Heparinized blood was collected from heart, and neutrophil was prepared. MPO release and superoxide generation were measured as described previously (Ishida-Okawara et al., 1991).

Measurement of proinflammatory cytokines and chemokine in plasma

Levels of proinflammatory cytokines IL-1β, IL-6, IL-10, IL-12, IL-18, TNF-α, INF-γ, MIP-2, soluble ICAM-1, G-CSF, GM-CSF in plasma using individual ELISA.

Preparation of peritoneal exudate neutrophils and measurement of cytokine production level by co-cultured neutrophil with CAWS

Normal C57BL/6N mice were intraperitoneally injected with 4 ml of 8% casein in PBS and exudate cells containing resident macrophage or casein-induced neutrophils were recovered 8 h lavage with 5 ml of PBS. The exudate cells were put onto M-SMF (Japan Immunoresearch Laboratories Co., Ltd., Takasaki, Japan), centrifuged 1200×g for 20 min at room temperature. Neutrophils were suspended (5×10^6 cells/ml) in RPMI-1640 medium containing 0.3 mM PMSF and 0.4 μg/ml aprotinin and co-cultured with 1 mg/ml CAWS for 0.5 to 4 h. At the end of culture, culture supernatant was prepared by centrifugation and levels of cytokines IL-1β, IL-6, IL-10 determined using by ELISA kits.

Measurement of ICAM-1 mRNA expressed in aortic wall after CAWS injection

The thoracic aortas of mice were was isolated and frozen immediately for detection of ICAM-1 mRNA. The total aortic RNA for each mouse was isolated using ISOGEN (Nippon ene, Tokyo Japan). One microgram of RNA was reverse transcribed with ReverTra Ace (Toyobo, Osaka, Japan) to obtain cDNA. Real-time PCR was performed using ABI PRISM 7000 Sequence Detection System (Applied Biosystems, CA, US) according to the manufacture's protocol. Primers and TaqMan probes specific for ICAM-1 was obtained from Assay-on-Demand Gene Expression Products (Applied Biosystems). For endogenous control, the level of GAPDH in each sample was measured using TaqMan Rodent GAPDH Control Reagents VIC (Applied Biosystems). Data analyses were performed on ABI PRISM 7000 SDS software version 1.0 (Applied Biosystems).

Detection of mouse complement 3 (C3) by ELISA and Western blotting

Peripheral blood was collected from heart and EDTA-2K was added. One μg/ml of C3 monoclonal antibody was coated to ELISA plate for overnight. After washing, blocking was done by 50% FCS for 1 h. Sample plasma (×100) was added to the plate for 1 h, after washing peroxidase labeled-2nd antibody (×1000) was added to the plate. After washing, *o*-phenylenediamine chloride was added to the plate for 3 min. Finally, reaction was stopped 2 N hydrogen sulphate and measured at 490 nm by auto reader (Nippon Bunko, Tokyo, Japan). Western blotting was performed by using mouse C3 monoclonal antibody and peroxidase-labeled anti-Rat IgG as 2nd antibody.

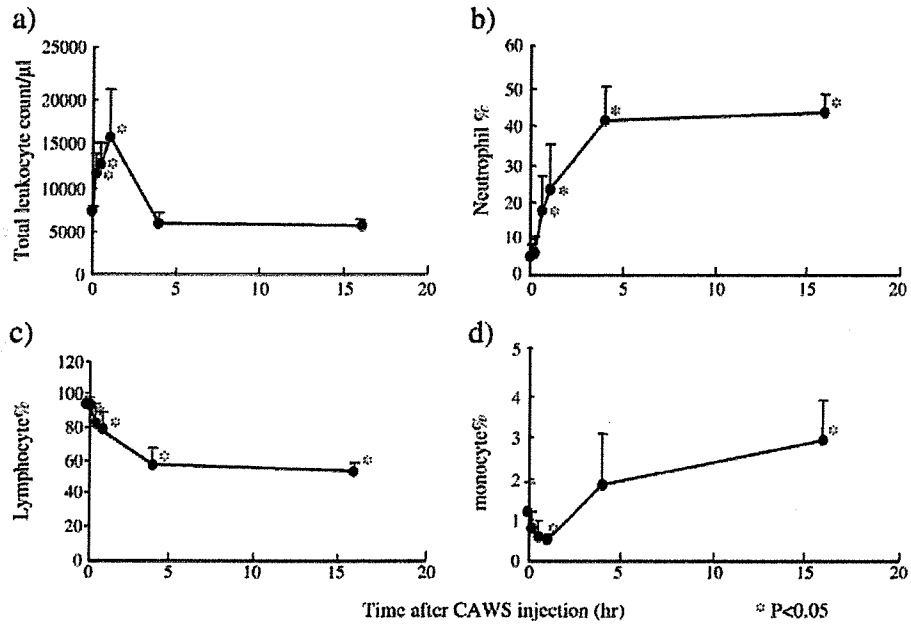

Fig. 2. Change of blood profile after CAWS injection. Peripheral blood was collected from heart EDTA-2K. Blood profile was analyzed by Mitsubishi Kagaku BCL Inc. (a) total leukocyte number, ratio of (b) neutrophil, (c) lymphocyte and (d) monocyte, respectively. $N=6$ in each group.

Table 1
Change of Gr-1$^+$ cells ratio after CAWS injection

	Time after CAWS injection (hr)					
	0	0.17	0.5	1	4	16
Bone marrow	19.47±5.35	15.85±1.89	9.65±1.14*	10.42±1.26*	7.39±1.97*	11.73±6.58
Peripheral blood	5.24±6.92	5.30±0.36	10.35±2.00*	9.78±3.59	8.06±6.69	6.12±5.34

* $P<0.05$.

Statistical analysis

Results expressed as the mean±SD. Statistical analysis was using Mann–Whitney *U*-test. The probability value of <0.05 considered significant.

Results

Observation of coronary arteritis administration of a single dose of CAWS

We have severe coronary arteritis by daily injection of CAWS (4 mg/mouse/day) for 5 days. In order to compare initial events and development of coronary arteritis, the current studies employed a one shot injection of CAWS at a dose of 4 mg/mouse. Four weeks after CAWS injection with this protocol, arteritis was evident in both coronary and aorta.

Profiles of peripheral leukocytes

After CAWS injection, total leukocyte counts were increased and later returned to baseline levels 4 h (Fig. 2a). The ratio of lymphocytes decreased after CAWS injection, while ratio of neutrophils promptly increased (Figs. 2b, c), the ratio of monocyte increased (Fig. 2d).

Profile of leukocyte by flow cytometric analysis

To confirm the leukocyte counts, flow cytometric analysis of peripheral and bone marrow cells after CAWS injection was done (Table 1). Bone marrow cell numbers the tibia were significantly increased 4 h after CAWS injection (data not shown). The ratio of Gr-1 cells in bone marrow significantly decreased at 0.5, 1, 4 h after CAWS injection, while the ratio of the cells in peripheral blood increased suggesting that neutrophils in bone marrow promptly migrate to peripheral blood CAWS injection.

CAWS effect on neutrophil activation

To the functional response of neutrophils after CAWS injection, MPO release and superoxide generation were

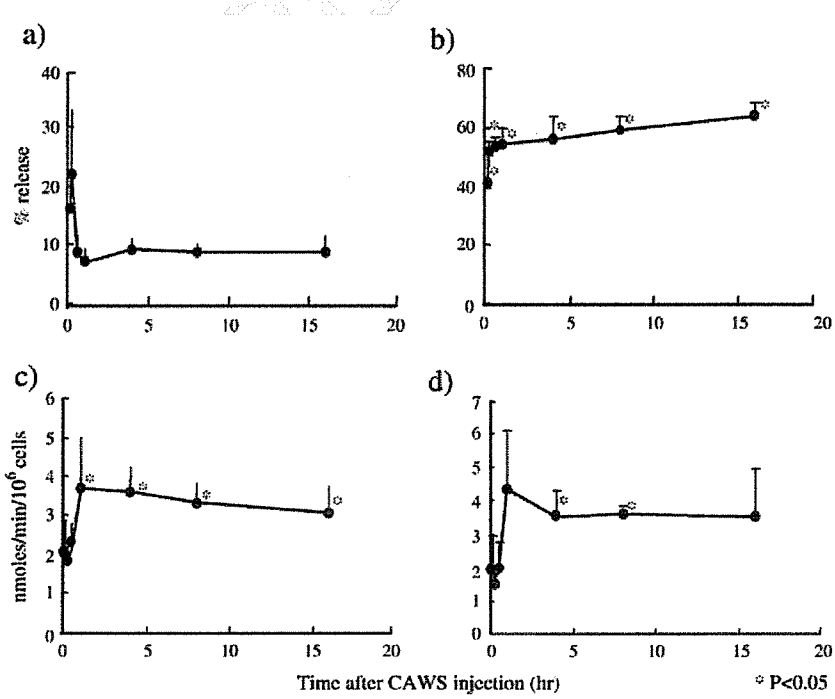

Fig. 3. Neutrophil activation after CAWS injection. (a, b) MPO release from neutrophils after CAWS injection. Neutrophils (10^6 cells/ml) were stimulated in the (a) absence, or (b) presence of (10^{-5} M) and (5 μg/ml). (c, d) Superoxide generation after CAWS injection. Neutrophils (10^6 cells/ml) were stimulated with (c) (10^{-5} M) and (5 μg/ml) or (d) PMA (1 μg/ml). $N=6$ in each group.

examined (Fig. 3). fMLP-induced MPO release from neutrophils was enhanced after CAWS injection (Fig. 3b), while spontaneous MPO release was not changed (Fig. 3a). In addition, both fMLP and PMA-induced superoxide generation was enhanced following in vivo CAWS injection (Figs. 3c, d).

CAWS effects on proinflammatory cytokine production

Since activation of neutrophils was observed, after in vivo injection of CAWS, proinflammatory cytokines levels in plasma were measured (Fig. 4). IL-12 p70 production was increased IL-1β (b), IL-10 (c), 1L-6 (d) significantly increased CAWS injection. Levels of MIP-2 and G-CSF in plasma increased after CAWS injection and 16 h after CAWS injection (Figs. 4e, f). On the other hand, IL-18, TNF-α, INF-γ, GM-CSF were not detected up to 16 h after CAWS injection (data not shown). Since IL-1β, IL-10, IL-6 was significantly increased, production of these cytokines by casein-induced neutrophils was also measured (Fig. 5). IL-6 production was enhanced by exposure of neutrophils to CAWS (Fig. 5c), while IL-11L-10 was nearly the same in presence or absence of CAWS (Figs. 5a, b).

CAWS effect of ICAM-1 expression and soluble ICAM release

Sine ICAM-1 is a marker of activation of endothelial cells, we ICAM-1 gradually increased in plasma after CAWS injection (Fig. 6a). In addition, ICAM-1 the thoracic aortic wall was also significantly increased 16 h after CAWS injection (Fig. 6b).

CAWS C3 activation

Activation of C3 was examined (Fig. 7). C3 decreased time dependently after CAWS injection and gradually (Fig. 7a). This was confirmed by Western blotting analysis (Fig. 7b). These results suggest that neutrophil activation triggered through complement activation by a single injection.

Discussion

In study, we focused on neutrophil activation related to development of coronary arteritis. Single injection of CAWS at a dose of 4 mg/mouse induced coronary arteritis 4 weeks featuring neutrophil accumulation in the coronary arterial wall. This observation was similar to the

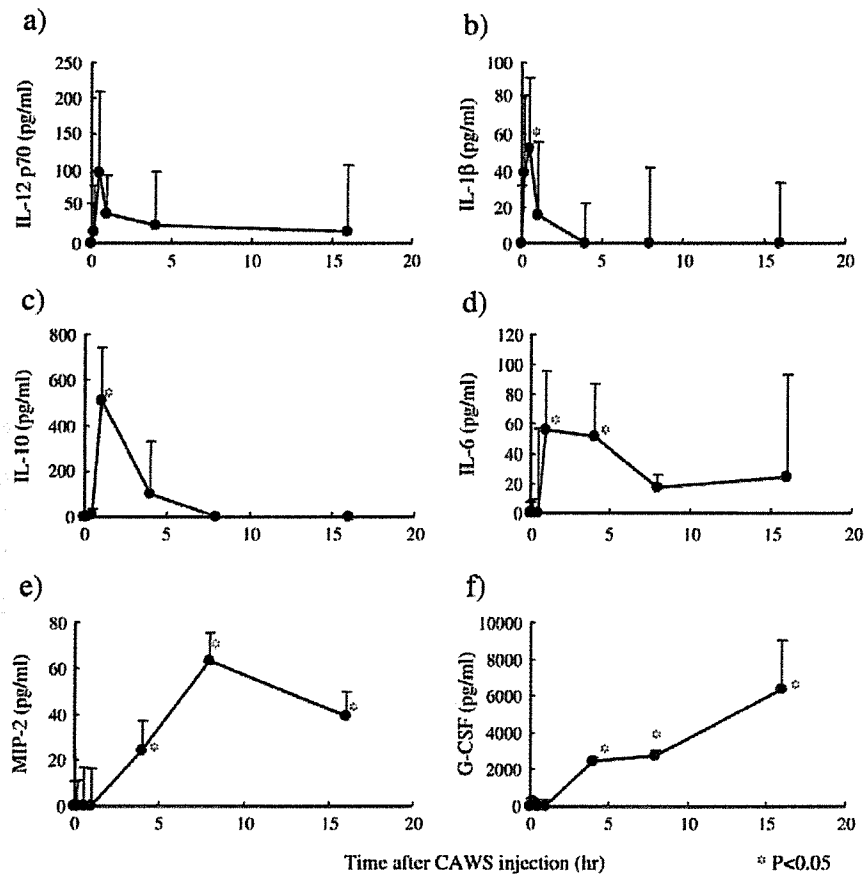

Fig. 4. Cytokine after CAWS injection. Heparinized blood was obtained from heart after CAWS injection. Plasma was separated and proinflammatory cytokines level was measured by ELISA kit. IL-12 p70, (b) IL-1β, (c) IL-10, (d) IL-6, (e) MIP-1, (f) G-CSF, respectively. $N=6$ in each group.

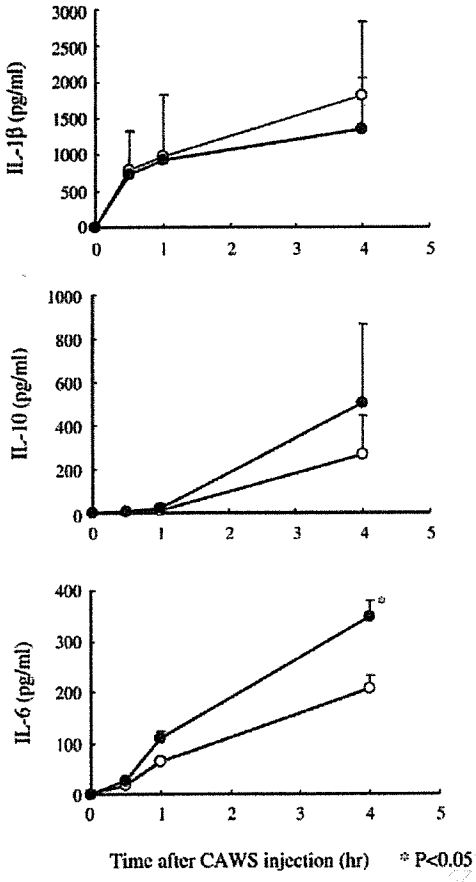

Fig. 5. Cytokine production by neutrophil. Casein-induced neutrophil (5×10^6 cells/ml) suspended in RPMI-1640 containing 0.3 mM PMSF and 1.4 μg/ml aprotinin and co-cultured with 1 mg/ml CAWS for 0.5 to 4 h. culture supernatant was prepared by centrifugation and level of cytokine. (a) IL-1β, (b) IL-10 and (c) IL-6, respectively. ○ not treated by CAWS ● 1 mg/ml of CAWS. N=3–6 in each group.

development of coronary arteritis daily injection of CAWS (4 mg/mouse/day) 5 days (Nagi-Miura et al., 2004; Ohno, 2003).

Blood neutrophils and subsequently monocyte increased, while lymphocyte counts decreased. In addition, the ratio of Gr-1 cells in bone marrow decreased, suggesting migration of neutrophils from bone marrow into peripheral blood after CAWS injection. G-CSF after CAWS injection, fMLP-induced MPO release from neutrophils was enhanced as was PMA and fMLP-induced superoxide generation in vivo injection. These results suggest that number of blood neutrophils their activation early after CAWS injection.

Levels of IL-1β, IL-6, and 1L-10 significantly increased in plasma after CAWS injection. These cytokines are also blood leukocytes live *C. albicans* (Netea et al., 2002; Gasparoto et al., 2004). The of cytokines seems to be different depend on *Candida* strain, component and virulence (Villar et al., 2005). With regard to casein-induced neutrophils, IL-6 was significantly enhanced by co-culture with CAWS, but IL-1β and 1L-10 production virtually unchanged in presence of CAWS. These results suggest IL-6 production especially enhanced by CAWS. MIP-2 and G-CSF in plasma were maintained for 16 h, neutrophil levels in blood MIP-2 and G-CSF in blood.

Because of increase and activation of peripheral neutrophils, complement activation products may well be candidate because C5a is a chemoattractant for neutrophils (Guo and Ward, 2005). Ohno et al. have already demonstrated activation of the lectin complement pathway by CAWS (unpublished). Mullick A. et al. have confirmed dysregulated cytokine response during *C. albicans* infection (Mullick et al., 2004).

Soluble ICAM-1, which is a marker of activated endothelial cells (Iiyama et al., 1999), in blood increased after CAWS injection. In addition, ICAM-1 message was significantly increased in the thoracic aortic wall 16 h after CAWS injection. Both systemic and local increases in ICAM-1 could be involved to subsequent endothelial cell lesion development (Di Lorenzo et al., 2004).

In summary, increased numbers and activation of peripheral blood neutrophils are the initial events after CAWS injection, perhaps followed by macrophage activation and adaptive immune responses. Neutrophil a primary role in biodefense

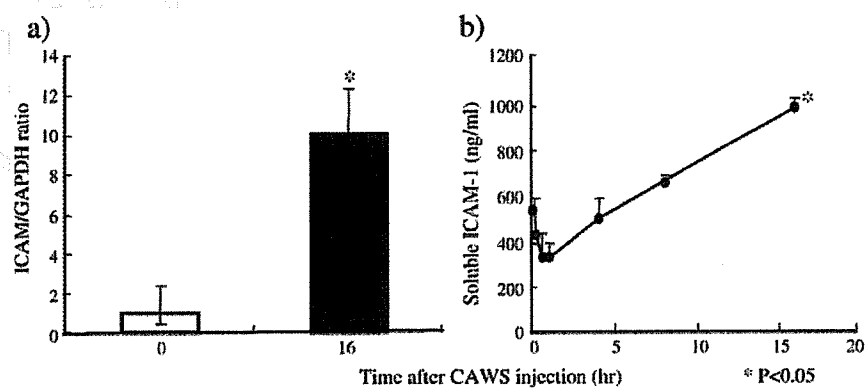

Fig. 6. Soluble ICAM-1 in plasma and ICAM-1 mRNA in aorta after CAWS injection. (a) Heparinized blood was obtained from heart after CAWS injection. Plasma was separated and ICAM-1level was measured by ELISA kit. (b) Total RNA was extracted and mRNA isolated. cDNA was prepared from 1 μg of mRNA. Real-time PCR was performed and analyzed. GAPDH was used as an internal control. White bar shows not treated by CAWS, black bar shows treated by 4 mg/mouse of CAWS, respectively. N=6 in each group.

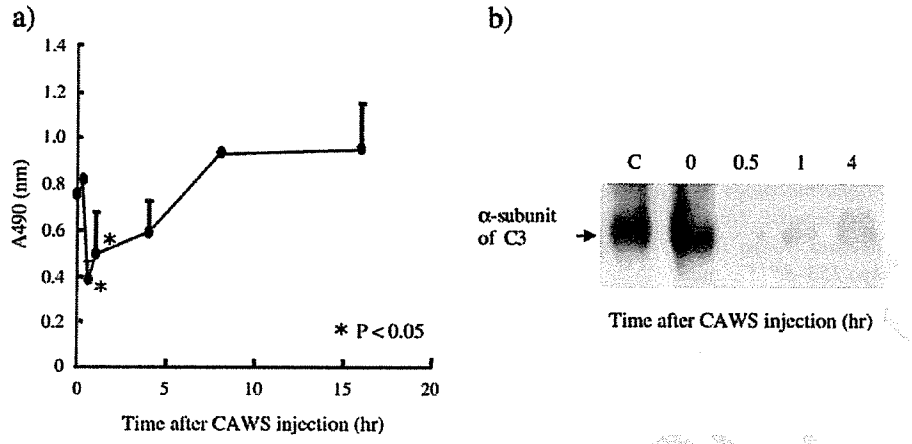

Fig. 7. Mouse complement 3 (C3) was assessed in plasma by sandwich ELISA and Western blotting. 10 mM EDTA treated blood was prepared from heart after CAWS injection. (a) C3 protein was detected by sandwich ELISA using monoclonal and peroxidase-labeled polyclonal antibody, (b) α chain of C3 was detected by monoclonal antibody to mouse C3.

against *C. albicans* or its products. Arteritis induced by CAWS might be.

Uncited reference

Collins et al., 2000

Acknowledgments

This work was supported in part by grants for vascular diseases from Ministry of Health Labor and Welfare of Japan and Japan Health Science Foundation.

References

Aratani, Y., Kura, F., Watanabe, H., Takano, Y., Suzuki, K., Dinauer, M.C., Maeda, N., Koyama, H., 2002. Relative contributions of myeloperoxidase and NADPH-oxidase to the early host defense against pulmonary infections with *Candida albicans* and *Aspergillus fumigatus*. Med. Mycol. 40, 557–563.

Collins, R.G., Velji, R., Guevara, N.V., Hicks, M.J., Chan, L., Beaudet, A.L., 2000. P-Selectin or intercellular adhesion molecule (ICAM)-1 deficiency substantially protects against atherosclerosis in apolipoprotein E-deficient mice. J. Exp. Med. 191, 189–194.

Di Lorenzo, G., Pacor, M.L., Mansueto, P., Lo Bianco, C., Di Natale, E., Rapisarda, F., Pellitteri, M.E., Ditta, V., Gioe, A., Giammarresi, G., Rini, G.B., Li Vecchi, M., 2004. Circulating levels of soluble adhesion molecules in patients with ANCA-associated vasculitis. J. Nephrol. 17, 800–807.

Esper, F., Shapiro, E.D., Weibel, C., Ferguson, D., Landry, M.L., Kahn, J.S., 2005. Association between a novel human coronavirus and Kawasaki disease. J. Infect. Dis. 191, 499–502.

Fradin, C., De Groot, P., Mac Callum, D., Schaller, M., Klis, F., Odds, F.C., Hube, B., 2005. Granulocytes govern the transcriptional response, morphology and proliferation of *Candida albicans* in human blood. Mol. Microbiol. 56, 397–415.

Gantner, B.N., Simmons, R.M., Underhill, D.M., 2005. Dectin-1 mediates macrophage recognition of *Candida albicans* yeast but not filaments. EMBO J. 24, 1277–1286.

Gasparoto, T.H., Gaziri, L.C., Burger, E., de Almedia, R.S., Felipe, I., 2004. Apoptosis of phagocytic cells induced by *Candida albicans* and production of IL-10. FEMS Immunol. Med. Microbiol. 42, 219–224.

Guo, R.F., Ward, P.A., 2005. Role of C5a in inflammatory responses. Annu. Rev. Immunol. 23, 821–852.

Iiyama, K., Hajra, L., Iiyama, M., Li, H., DiChiara, M., Medoff, B.D., Cybulsky, M.I., 1999. Patterns of vascular cell adhesion molecule-1 and intercellular adhesion molecule-1 expression in rabbit and mouse atherosclerotic lesions and at sites predisposed to lesion formation. Corc. Res. 85, 199–207.

Ishida-Okawara, A., Kimoto, Y., Watanabe, K., Shibata, M., Masuda, K., Takano, Y., Kawaguchi, K., Akagawa, H., Nilubol, N., Hotta, K., Yazawa, K., Mizuno, S., Suzuki, K., 1991. Purification and characterization or aseanostains: actinomycete-derived fatty acid inhibitors to myeloperoxidase release from human polymorphonuclear leukocytes. J. Antibiot. 44, 524–532.

Iwai, T., Inoue, Y., Umeda, M., Huang, Y., Kurihara, N., Koike, M., Ishikawa, I., 2005. Oral bacteria in the occluded arteries of patients with Buerger disease. J. Vasc. Surg. 42, 107–115.

Muller, J., Melchinger, W., 2004. The significance of *Candida* serology based on cell wall antigens. Mycoses 47, 2–10.

Mullick, A., Elias, M., Picard, S., Bourget, L., Jovecevski, O., Gauthier, S., Tuite, A., Harakidas, P., Bihun, C., Massie, B., Gros, P., 2004. Dysregulated inflammatory response to *Candida albicans* in a C5-deficient mouse strain. Infect. Immun. 72, 5868–5876.

Nagi-Miura, N., Shingo, Y., Adachi, Y., Ishida-Okawara, A., Oharaseki, T., Takahahi, K., Naoe, S., Suzuki, K., Ohno, N., 2004. Induction of coronary arteritis with administration of CAWS (*Candida albicans* water-soluble fraction) depending on mouse strains. Immunopharmacol. Immunotoxicol. 26, 527–543.

Netea, M.G., Stuyt, R.J., Kim, S.H., Van der Meer, J.W., Kullberg, B.J., Dinarello, C.A., 2002. The role of production of interferon-gamma induced by *Candida albicans* in human whole-blood cultures. J. Infect. Dis. 185, 963–970.

Ohno, N., 2003. Chemistry and biology of angitis inducer. *Candida albicans* water-soluble mannnoprotein-beta-glucan complex(CAWS). Microbiol. Immunol. 47, 479–490.

Spellberg, B.J., Collins, M., French, S.W., Edwards Jr., J.E., Fu, Y., Ibrahim, A.S., 2005. A phagocytic cell line markedly improves survival of infected neutropenic mice. J. Leukocyte Biol. 78, 338–344.

Takahashi, M., Koga, M., Yokoyama, K., Yuki, N., 2005. Epidemiology of *Campylobacter jejuni* isolated from patients with Guillain–Barre and Fisher syndromes in Japan. J. Clin. Microbiol. 43, 335–339.

Urban, C.F., Reichard, U., Brinkmann, V., Zychlinsky, A., 2006. Neutrophil extracellular traps capture and kill *Candida albicans* yeast and hyphal forms. Cell. Microbiol. 8, 668–676.

Villar, C.C., Kashleva, H., Mitchell, A.P., Dongari-Bagtzoglou, A., 2005. Invasive phenotype of *Candida albicans* affects host proinflammatory response to infection. Infect. Immun. 73, 4588–4595.

Zupanic-Krmek, D., Nemet, D., 2004. Systemic fungal infections in immunocompromised patients. Acta Med. Croat. 58, 251–261.

Highlighted paper selected by Editor-in-chief

Beta-Mannosyl Linkages Negatively Regulate Anaphylaxis and Vasculitis in Mice, Induced by CAWS, Fungal PAMPs Composed of Mannoprotein–Beta-Glucan Complex Secreted by *Candida albicans*

Hiroyasu SHINOHARA,[a] Noriko NAGI-MIURA,[a] Ken-ichi ISHIBASHI,[a] Yoshiyuki ADACHI,[a] Akiko ISHIDA-OKAWARA,[b] Toshiaki OHARASEKI,[c] Kei TAKAHASHI,[c] Shiro NAOE,[c] Kazuo SUZUKI,[b] and Naohito OHNO*,[a]

[a] *Laboratory for Immunopharmacology of Microbial Products, School of Pharmacy, Tokyo University of Pharmacy and Life Science; 1432–1, Horinouchi, Hachioji, Tokyo 192–0392, Japan:* [b] *Department of Bioactive Molecules, National Institute of Infectious Diseases; Tokyo 162–8640, Japan: and* [c] *Department of Pathology, Ohashi Hospital, Toho University School of Medicine; Tokyo 153–8515, Japan.*

Received April 19, 2006; accepted June 22, 2006; published online June 23, 2006

***Candida albicans* water soluble fraction (CAWS) is a water-soluble extracellular mannoprotein–beta-glucan complex obtained from the culture supernatant of *Candida albicans*, which grows in a chemically defined medium. CAWS induced toxic reactions, such as acute anaphylactoid reaction, by intravenous administration and coronary arteritis by intraperitoneal administration. To clarify the structure responsible for these toxic reactions, *C. albicans* was cultured in pH- and temperature-controlled conditions and prepared with CAWS with or without the beta-1,2-linked mannosyl segment (BM). The structure of CAWS was assessed by immunochemical and spectroscopic methodologies, and we found that CAWS prepared under the natural culture conditions contained only small amounts of BM and CAWS prepared at neutral conditions at 27 °C contained a significantly higher percentage of BM. Both the acute lethal toxicity and coronary arteritis induction was significantly more severe in the absence of BM. Activation of a complement pathway, the lectin pathway, by CAWS was significantly stronger in the absence of BM. These facts strongly suggest that BM linkages in CAWS negatively modulate acute and chronic toxicity of CAWS, and may be strongly related to the lectin pathway of the complement activation.**

Key words *Candida albicans*; arteritis; mannoprotein; beta-1,2-mannan; DBA/2 mice

Candida spp. is a medically important fungus that frequently induces deep mycosis and fungemia, especially in immunocompromised hosts.[1] Pathogenic microbes have various toxic mechanisms that are unique to each species and are essential for survival and evolution. Pathogenic mechanisms of eukaryotic microbes are complicated compared to those of bacteria and viruses. Although there have been extensive basic and clinical studies, the major pathogenic factors for *Candida* spp. are still unknown and precise characterization of each of the constituents would be valuable.

Cardiovascular disease is one of the most life-threatening diseases, and various new compounds and new methods of pharmaceutical care, such as gene therapy and drug delivery systems, have been developed to treat it. There are several lines of evidence suggesting that inflammatory cells, particularly macrophages and neutrophils, regulate endothelial cell function and dysfunction in atherosclerosis, *via* the release of mediators that display proinflammatory activity. Analysis of such diseases by animal models will give promising feedback to human health.

Murata *et al.*[2] reported that Kawasaki-disease-like coronary arteritis was induced in mice by administration of an alkaline extract of *C. albicans* (CADS) isolated from patients with Kawasaki disease (KD). KD, a disease of unknown cause that mainly affects children aged 4 and under, was first reported by Kawasaki in 1967.[3] The patient presents with systemic coronary arteritis in nearly 10% of cases. Although the occurrence of such coronary artery disorders has decreased with γ-globulin therapy, the mechanism of occurrence along with the pharmacological mechanism of treatment is unknown.[4] Murata's murine model has been extensively examined from various points of view, *e.g.* anti-myeloperoxidase antibody production, susceptibility loci, and histopathological features.[5,6]

Previously, we prepared a water-soluble polysaccharide fraction of *C. albicans* released into a culture supernatant (*Candida albicans* water-soluble fraction: CAWS) and performed various analyses.[7—10] The most important point concerning this system is that we use a completely synthetic medium, named C-limiting medium, to eliminate contaminants from the culture medium, such as endotoxins, peptidoglycans, and nucleic acids. Series of our studies found that CAWS shows various toxic activities, such as cytokine synthesis by leukocytes, platelet aggregation, lethal toxicity, enhancement of side effect of indomethacin, induction of coronary arteritis in mice, and so on. Thus, CAWS may be a pathogen-associated microbial product (PAMPs) of *Candida albicans*.

In a previous study we found that intraperitoneal administration of CAWS to mice induces coronary arteritis similar to that induced by CADS.[8—10] It is of note that CAWS-induced arteritis showed significant strain dependency: The incidence of arteritis was 100% in C57BL/6, C3H/HeN and DBA/2 mice, but only 10% in CBA/J mice. The coronary arteritis observed in DBA/2 mice was the most serious, with the majority of mice expiring during the observation period.

The coronary arteritis induced by CAWS was accompanied by hypertrophy of the tunica intima, the rupture of elastic fibers and a diffuse invasion by lymphocytes, histiocytes, fibroblasts, smooth muscle cells and eosinophils of vascular

* To whom correspondence should be addressed. e-mail: ohnonao@ps.toyaku.ac.jp

endothelial cells and the regions surrounding blood vessels. Based on such characteristics, the coronary arteritis induced by CAWS was presumed to be proliferative granulomatous coronary arteritis, and is clearly different from fibrinoid arteritis. In DBA/2 mice, it was observed to cover nearly the entire periphery of the vessels, and those mice were considered to demonstrate the most virulent form of coronary arteritis.

Structure of yeast cell wall, such as in *Saccharomyces cerevisiae*, *Candida albicans*, and *Schizosaccharomyces pombe*, have been extensively examined and it was found that the overall structure is quite complex and regulated by expression of multiple genes.[11,12] According to the results of NMR and biochemical analyses, CAWS was found to be composed of a mannoprotein and β-glucan portion, which are the main components of the *C. albicans* cell wall.[8] The mannoprotein region of *Candida albicans* is composed of both *N*- and *O*-glycosyl linkages with alfa- and beta-linked mannosyl residues.[13,14] Phosphodiester linkages are also included. Mannan synthesis is regulated by several specific glycosyl transferases.[15—17] It is also an immunochemical determinant of *Candida* spp.[18,19] It is of note that the structure of mannan is modulated by various culture conditions, such as temperature and pH.[20,21] The structure of mannan is also known to be modulated by various stresses. The structure of mannan is a key molecule for recognition of *Candida* by host biodefense system and might be strictly regulated by the affinity for specific receptors. Analysis of the disease from the structural point of view is an indispensable study.

In a preliminary experiment, the pH of a culture medium was measured and it was found that shifted from 5.2 to 2.3 at the end. In the present study, we have prepared CAWS using different culture conditions and examined CAWS-induced anaphylactoid reaction and vasculitis. We demonstrated that beta-1,2-mannosyl linkages are the negative regulators for both anaphylactoid reaction and vasculitis.

MATERIALS AND METHODS

Mice Male ICR and DBA/2 mice were purchased from Japan SLC. The mice were housed in a specific pathogen-free (SPF) environment and were used in the study at 5 weeks of age. All animal experiments were followed by the guideline of laboratory animal experiments in Tokyo University of Pharmacy and Life Sciences (TUPLS), and each of the experimental protocol was approved by the committee of laboratory animal experiments in TUPLS.

Preparation of CAWS *Candida albicans* strain IFO1385 was purchased from the Institute for Fermentation, Osaka (IFO), stored at 25 °C on Sabauroud's agar (Difco, U.S.A.) and passaged once every three months. CAWS was prepared from *C. albicans* strain IFO1385 in accordance with conventional methods.[7,9,10] The procedure used was as follows: 5 l of medium (C-limiting medium) was added to a glass incubator and cultured for 2 d at 27 °C with air supplied at a rate of 5 l/min and rotation at 400 rpm. Following the culture, an equal volume of ethanol was added and after the mixture was allowed to stand overnight, the precipitate was collected. The precipitate was dissolved in 250 ml of distilled water, ethanol was added and the mixture was allowed to stand overnight. The precipitate was collected and dried with acetone to obtain CAWS.

Administration Schedule for Induction of Coronary Arteritis (10) CAWS (4 mg/mouse) was administered intraperitoneally for 5 consecutive days to each mouse in week 1. At week 5, the hearts of the animals were fixed with 10% neutral formalin and prepared in paraffin blocks. Tissue sections were stained with hematoxylin–eosin (HE) stain.

ELISAs of *Candida* Typing Sera to CAWS The reactivity of CAWS to serum factors from *Candida* that consists of rabbit polyclonal antibodies against *Candida* cell wall mannan was detected by ELISA. A solution of CAWS in 50 mM carbonate buffer (pH 9.6) was coated onto Nunc immunoplates, which were then incubated at 4 °C overnight. The plates were washed extensively with 0.05% Tween 20 containing PBS (PBST); unbound sites were blocked by the addition of 1% BSA containing PBST (BPBST) to wells for 40 min at 37 °C and then the wells were washed 6 times with PBST. *Candida* serum factors serially diluted with BPBST were added, and incubated for 60 min at 37 °C. After 6 washes with PBST, the wells were treated with peroxidase-conjugated goat anti-rabbit IgG and the 3,3′,5,5′-tetramethylbenzidine microwell peroxidase substrate system (TMB; KPL inc). After 45 min, the reaction was stopped with 1 N H_3PO_4, and then the optical density of each well was read at 450 nm on an automatic microplate reader.

Measurement of Complement Activation The complement kit for assessment of classical, alternative and MBL pathway activity was developed by the EU consortium and is now commercially available (Wielisa COMPL300 Total Complement Functional Screen kit from Wieslab AB, Lund, Sweden). The kit was operated by the instructions provided in the manual with slight modifications. In brief, strips of wells for classical pathway (CP) evaluation were precoated with IgM, strips for alternative pathway (AP) determination were coated with LPS, and mannose binding lectin (MBL) pathway (MBL-P) strips were coated with mannan. Sera were diluted 1/101 for the CP and MBL-P assay and 1/18 for the AP assay in specific buffers, serial dilutions of CAWS solution was added to the diluted sera and incubated. The resulting sera were added to the strips of the kit and were incubated for 1 h at 37 °C. After washing the strips, alkaline phosphatase-conjugated antihuman C5b-9 was added and incubated at room temperature for 30 min. Additional washing was performed, substrate was added, and the wells were incubated for 30 min. Finally, absorbance values were read at 405 nm. In each assay, standard positive and negative control sera provided in the kit as lyophilised material were reconstituted with distilled water. Complement activity was calculated using the following formula: activity=100%×(mean A405 (sample)−mean A405 (negative control)/(mean A405 (standard serum)−mean A405 (negative control). Samples as well as standard serum and negative control serum were tested in duplicate at a fixed dilution.

Assay for Anaphylactoid Reaction Indicated dose of CAWS solution was i.v. administered to ICR mice. The incidence and the severity of the rapid anaphylactoid shock were assessed within 30 min. For measuring tolerance, low dose CAWS was i.v. administered to ICR mice 1 h prior to induce anaphylactoid reaction by CAWS (400 μg/mouse).

NMR Spectroscopy H1-NMR experiments were performed with a Bruker DPX 400 equipped with XWIN-NMR

software. The spectra were recorded using a solution of each soluble fraction (10 mg/ml) in D_2O at 45 °C with acetone as an internal standard.

RESULTS

Preparation of CAWS by Various Culture Conditions Figure 1 shows the data of pH monitoring during *Candida* culture in C-limiting medium. The data clearly demonstrated that at pH uncontrolled natural time course, pH was 5.2 at the beginning and was lowered to around 2 at the end, thus the naturally expressed CAWS was produced in this culture condition. In order to prepare CAWS with modulated mannan structure, *C. albicans* IFO1385 was cultured at either 27 °C or 37 °C in C-limiting medium. In addition, pH of the culture medium was controlled at either pH 2.3, 5.2, or 7.0 by automatically added sodium hydroxide solution. The extracellular mannoprotein fraction was prepared by a previously established procedure that was the same as naturally produced CAWS. The names of each fraction were designated as CAWS 27-2.3, CAWS 27-5.2, CAWS 27-7.0, CAWS 37-2.3, CAWS 37-5.2, and CAWS 37-7.0. The name of CAWS prepared at natural pH course was designated as 27-(–) and 37-(–), respectively. In addition, CAWS prepared at 27 °C was designated as CAWS 27s which include 27-2.3, 27-5.2, 27-7.0, and 27-(–), and prepared at 37 °C as CAWS 37s which include 37-2.3, 37-5.2, 37-7.0, and 37-(–). Yield and some parameters of each CAWS are shown in Table 1. The structure of the mannan moiety was characterized by the reactivity to the typing sera and NMR spectral analysis.

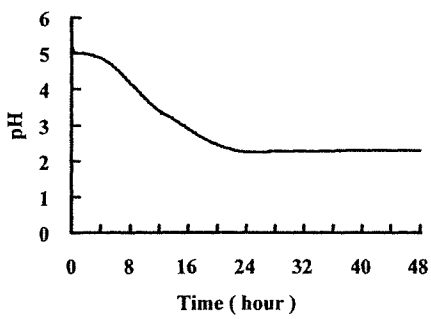

Fig. 1. Monitoring pH of *C. albicans* IFO1385 Culture in C-Limiting Medium at 27 °C

One hundred milliliters of *C. albicans* IFO1385 precultured in liquid to logarithmic phase was added to 4 l of C-limiting medium in a jar fermenter with 4 l air/min and 400 rpm stirring. The pH of the culture medium was measured automatically with a pH meter.

Figure 2 shows relative reactivity to the typing sera no. 5, 6, and 11. Experiments were done using three doses of CAWS solution adsorbed onto the ELISA plates. The pattern of reactivity of each CAWS preparation to the sera were similar between no. 5 and no. 6. In contrast, reactivity to no. 11 was significantly different. In the cases of no. 5 and no. 6, comparing the dose to show absorbance 1.0, reactivity of CAWS 27-5.2 and CAWS 27-7.0 was significantly increased compared to CAWS 27-(–), and other preparations. In contrast, relative activity of CAWS 27-5.2 and CAWS 27-7.0

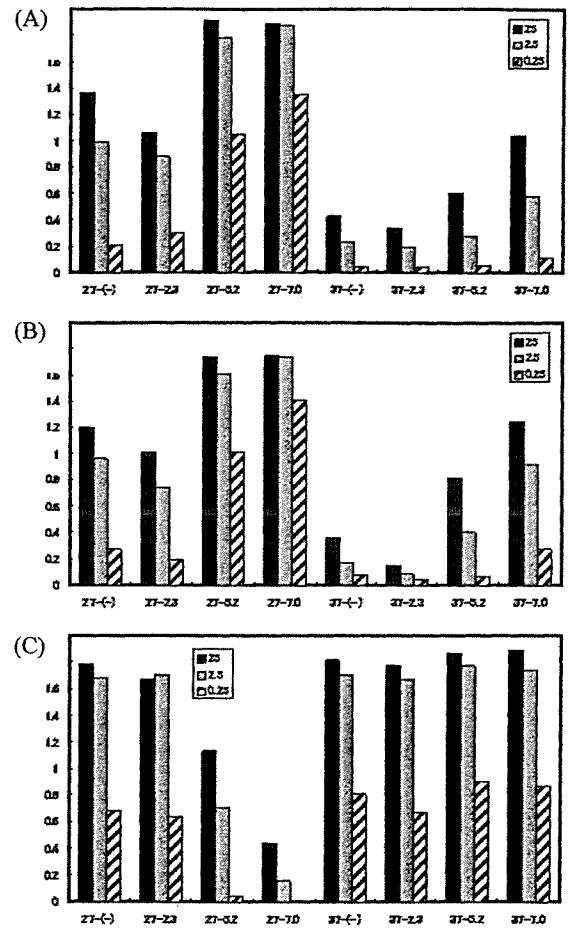

Fig. 2. Reactivity of CAWS Prepared under Various Conditions to *Candida* Typing Sera no. 5, 6, and 11

Each 25, 2.5, or 0.25 μg/ml solution of CAWS was adsorbed on ELISA plate and diluted typing sera was added. After appropriate incubation time, plate-bound antibody was measured by peroxidase conjugated anti-rabbit IgG with TMB reagent. (A) Anti no. 5; (B) anti no. 6; (C) anti no. 11.

Table 1. Properties of CAWS Prepared by Various Culture Conditions

CAWS	Yield (mg/l)	Cell (g/l)	C (%)	H (%)	N (%)	Factor G	Factor C
27-(–)	147±30	4.3±0.7	30.1±2.7	5.5±0.4	1.6±0.3	—	<2
27-2.3	132±19	4.0±0.2	27.5±4.7	5.0±0.7	1.6±0.1	0.73±0.57	0.25±0.1
27-5.2	247±26	3.5±0.4	28.6±3.5	5.2±0.4	2.8±0.3	ND	0.33±0.45
27-7.0	381±77	3.4±0.1	18.1±5.3	4.0±0.8	2.1±0.6	ND	0.71±0.73
37-(–)	84±33	2.0±0.7	26.5±1.8	4.8±0.4	1.1±0.1	1.24±0.21	0.03±0.02
37-2.3	160±17	3.3±0.1	18.5±9.1	3.7±1.5	1.1±0.2	0.56±0.16	ND
37-5.2	255±87	3.0±0.2	20.3±2.7	4.0±0.7	0.9±0.2	ND	0.1±0.03
37-7.0	263±12	3.2±0.5	24.3±1.1	4.9±0.1	1.5±0.1	0.07±0.01	0.08±0.01

27-(–); cultured at 27 °C without pH control, 27-2.3; cultured at 27 °C and pH was maintained at 2.3, 27-5.2; cultured at 27 °C and pH was maintained at 5.2, 27-7.0; cultured at 27 °C and pH was maintained at 7.0, cell; yield of dried cells. C, H, N; elemental analysys (carbon, hydrogen, nitrogen), factor G; content of 1,3-beta-glucan (ng/ml), factor C; content of endotoxin (ng/ml), ND; not detected.

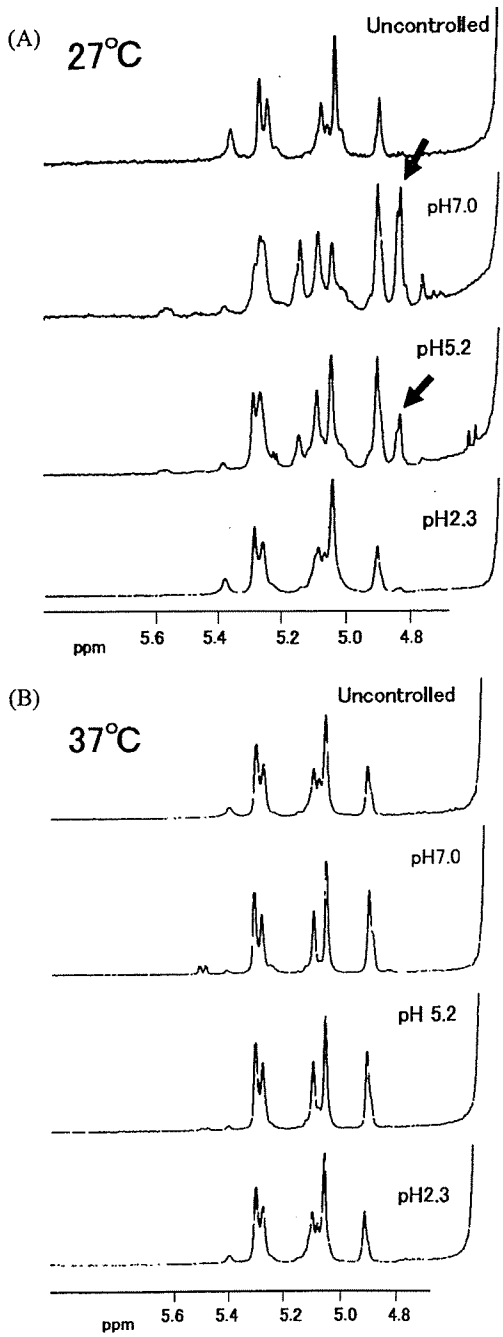

Fig. 3. Proton-NMR Spectra of CAWS in D_2O

(A) CAWS 27s prepared from the 27 °C culture. (B) CAWS 37s prepared from the 37 °C culture. Arrow indicates signals corresponding to beta-1,2-mannosyl linkages.

was significantly decreased in the case of typing sera no. 11. It is proposed that the specific epitope of no. 5 and no. 6 are for the beta-1,2-linked mannooligosaccharides, and no. 11 for the alpha-1,2 and 1,6-mannooligosaccharides.[20,21] These data strongly suggested that CAWS 27-5.2 and CAWS 27-7.0 contained significantly higher concentration of beta-1,2-linkages and reduced concentration of alfa-linkages.

Figure 3 shows NMR spectra of CAWS preparations. Each of the spectra contained many signals in the anomeric region (4.8—5.5), and thus, we could not do complete assessment at this time. However, comparing the published spectra of the cell wall mannan moiety of *Candida* spp. by Professor Suzuki *et al.*,[20,21] major signals could be assigned. Chemical shift around 4.85, shown as arrow in the spectra, would be beta-linked manno-oligosaccharides. The signal around 4.85 was only detected in the spectra of CAWS 27-5.2 and CAWS 27-7.0. Signals around 5.13 also appeared in those spectra would be the residues linked to beta-mannosyl linkages. In contrast, signals around 5.05 which include alpha-mannose residues was reduced in relation to the substitution of beta-mannosyl linkages. It is of note that even in the same pH conditions, CAWS 37-5.2 and CAWS 37-7.0 did not show such signals, and this observation was strongly supported by immunochemical reactivity. NMR spectra of CAWS 37-(–), CAWS 37-2.3, CAWS 37-5.2, and CAWS 37-7.0, shown in Fig. 3b show simple anomeric signals compared to those of CAWS 27s. Shibata *et al.* examined the cell wall mannan structure of *Candida parapsilosis* and *Candida albicans* by use of controlled hydrolysis and NMR spectroscopy.[22] Comparing Proton NMR spectra of *C. parapsilosis* and *C. albicans*, that of *C. parapsilosis* is simple and shows only 5 major signals in the anomeric region of 1D-NMR spectrum. Those signals correspond to alpha mannosyl linkages. At least in 1D-NMR spectrum, CAWS 37s resembles that of *C. parapsilosis*, also supporting that beta-1,2-linkages are missing in CAWS 37s. Regulation of beta-1,2-mannosyl linkages by culture condition is also reported in *Candida guilliermondii*.[23] From the data of immunochemistry and NMR spectra, CAWS 27-5.2 and CAWS 27-7.0 contained significantly higher concentrations of beta-1,2-linked manno-oligosaccharides.

Table 2. Anaphylactoid Reaction Induced by CAWS Prepared under Various Conditions

CAWS	3200	800	200	50	12.5
27-(–)			3/3	0/3	
27-2.3			3/3	0/3	
27-5.2	2/3	0/3	0/3		
27-7.0	0/3	0/3	0/3		
37-(–)			2/3	1/3	0/3
37-2.3			3/3	1/3	0/3
37-5.2			2/3	0/3	
37-7.0			2/3	0/3	

Indicated dose (μg/mouse) of CAWS was i.v. administered to mice (n=3). Lethality of each mouse was monitored 30 min later. */*, number of mice, dead/total.

Acute Toxicity of CAWS Prepared by Various Culture Conditions We have previously shown that CAWS induced acute anaphylactoid reaction, similar to *E. coli* O9 LPS and yeast mannan.[24,25] We compared acute anaphylactoid reaction of various CAWS preparations. As shown in Table 2, various concentrations of CAWS were intravenously administered to ICR mice and survival within 30 min was compared. In this experiment, the majority of CAWS preparations induced almost complete lethal toxicity at doses of 200 μg/mouse. However, CAWS 27-5.2 required 3200 μg for lethal toxicity and CAWS 27-7.0 did not show any lethal toxicity in this experimental condition. These facts strongly suggested beta-1,2-linked manno-oligosaccharide would be a negative regulator for acute anaphylactoid reaction. To confirm the possibility, tolerance induction by CAWS preparations was also tested. As shown in Table 3, administration of 16 μg of CAWS 27-(–) and CAWS 27-2.3 significantly reduced lethality of subsequent high dose CAWS administration. However, in the case of CAWS 27-5.2, a relatively

Table 3. Tolerance Induction in CAWS Induced Anaphylactoid Reaction by Pretreatment with CAWS Prepared under Various Conditions

CAWS	64	16	4	1
27-(–)		1/3	3/3	
27-2.3		0/3	2/3	2/3
27-5.2	0/3	2/3	2/3	

Indicated dose of CAWS (μg/ml) was i.v. administered to mice (n=3). CAWS-(–) was again i.v. administered to each mouse, and lethality was monitored 30 min later. */*, number of mice, dead/total.

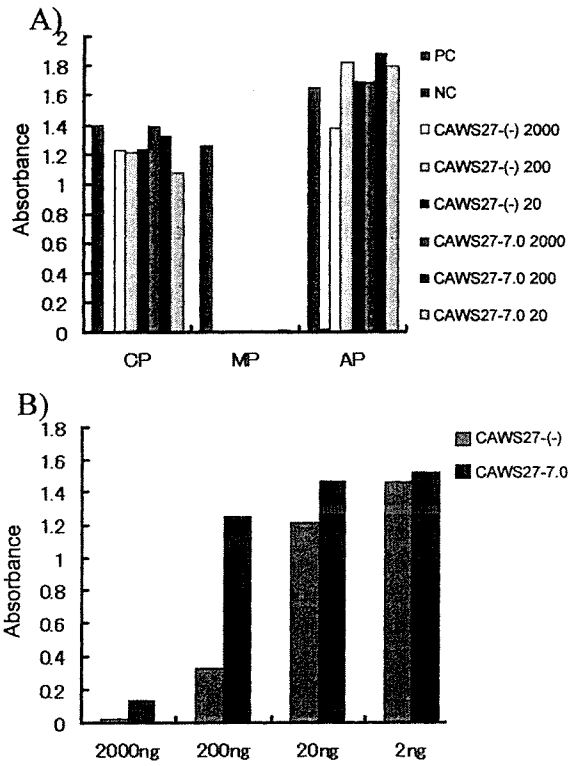

Fig. 4. Complement Activation by CAWS

(A) Screening of classical (CP), lectin (MP), and alternative (AP) pathway of complement activation by CAWS. (B) Dose response of CAWS-induced activation of the lectin pathway of complement. CAWS 27-(–) and CAWS 27-7.0 were used in this experiment. PC; positive control serum, NC; negative control serum.

higher dose, 64 μg, was required for tolerance induction. This result also strongly suggested that beta-1,2-mannooligosaccharides negatively modulate acute lethal toxicity of CAWS.

Complement activation and the resulting anaphylactic peptides, C3a and C5a, production are the most commonly postulated mechanism for acute toxicity. In the preliminary experiments, incubation of CAWS with human sera produced high concentration of C5a anaphylatoxic peptide. Because of the difficulty in measuring mouse complement activation, we used a commercially available kit for human complement activation in the present study. Activity of classical, lectin, and alternative pathways were measured using IgM, mannan, and LPS-coated ELISA plate and specific reaction buffer systems. As shown in Fig. 4a, CAWS of 20 to 2000 μg/ml were added, and it was found that CAWS activated complement was almost specifically mediated by the lectin pathway. In this dose range, CAWS 27-(–) and CAWS 27-7.0 did not show any differences; however, comparing the activity between doses of 20 ng and 200 ng shown in Fig 4b, CAWS 27-(–) showed almost ten times higher activity than CAWS 27-7.0. These results strongly suggest that beta-1,2-linked mannooligosaccharides inhibited complement activation by alfa-linked mannose residues.

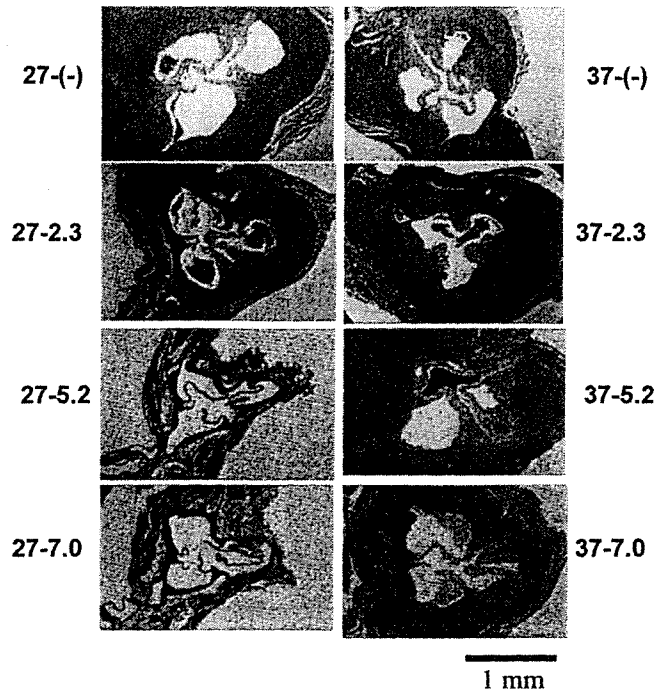

Fig. 5. Histological Analysis of DBA/2 Mice Administered with CAWS

CAWS prepared under various conditions (4 mg/mouse) was administered i.p. to DBA/2 mice for five consecutive days. Five weeks later, the aorta with coronary of these mice were stained with hematoxylin–eosin.

Arteritis Induction by CAWS Prepared by Various Culture Conditions Intraperitoneal injection of CAWS induced coronary arteritis in mice.[8—10] Severity is significantly dependent on strains of mice and DBA/2 shows the most severe reaction, resulting in death. Coronary arteritis induction by CAWS prepared as above was compared. CAWS was administered i.p. to each mouse at 4 mg/mouse for 5 consecutive days and sections of coronary artery were prepared at 4 weeks after the final CAWS administration. Figures 5 to 8 show hematoxylin eosin staining of aorta, aortic valve, and the coronary artery in CAWS-administered mice. CAWS prepared by the standard protocol induced strong inflammation in this area. CAWS 27-2.3, CAWS 37-(–), CAWS 37-2.3, CAWS 37-5.2, and CAWS 37-7.0 show similar inflammation. However, CAWS 27-5.2 and CAWS 27-7.0, both of which contained higher content of beta-1,2-manno-oligosaccharides, show significantly weaker inflammation. The histology of the aorta, aortic valve, and coronary artery using higher magnification (Figs. 7, 8) shows similar phenotypes.

Coronary arteritis was also examined by survival. As shown in Fig. 9, almost all of the mice that had CAWS administered died except for CAWS 27-5.2, in which only one mouse out of five died. Figure 10 shows the dose response of survival and corresponding histology of DBA/2 mice administered CAWS 27-(–). Arteritis was induced even with 250 μg/mouse administration and 2/5 mice died in this condition. Considering the data of survival and histology of CAWS 27-(–) and CAWS 27-5.2, the relative activity of

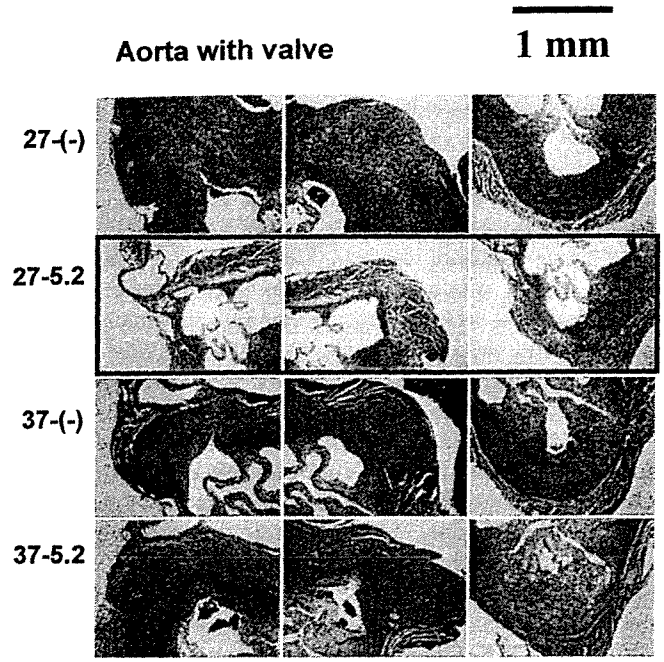

Fig. 6. Comparison of Histology of Aorta in DBA/2 Mice Administered Native and pH-Controlled CAWS

CAWS 27-(–), CAWS 27-5.2, CAWS 37-(–), CAWS 37-5.2 (4 mg/mouse) were administered i.p. to DBA/2 mice for five consecutive days. Five weeks later, the aorta with coronary of these mice were stained with hematoxylin–eosin.

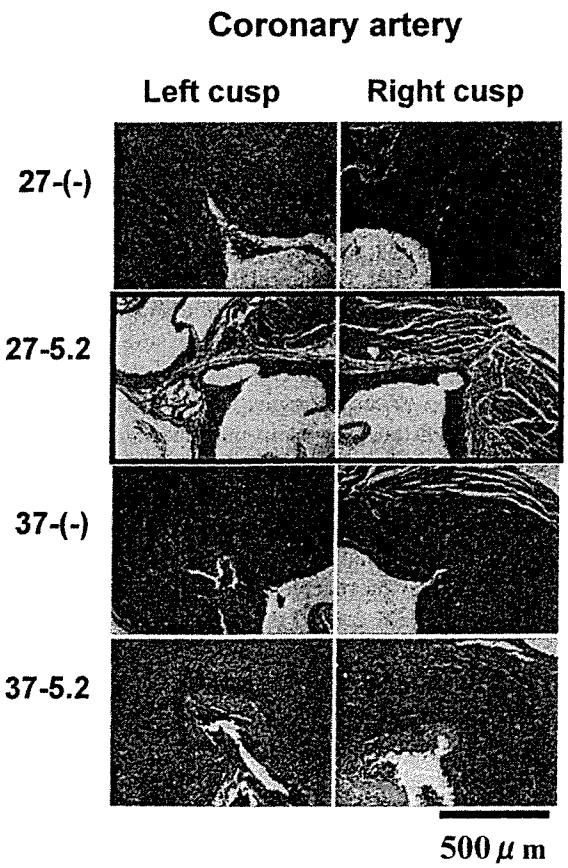

Fig. 7. Comparison of Histology of Cusp Region of Coronary Artery in DBA/2 Mice Administered Native and pH-Controlled CAWS

CAWS 27-(–), CAWS 27-5.2, CAWS 37-(-), CAWS 37-5.2 (4 mg/mouse) were administered i.p. to DBA/2 mice for five consecutive days. Five weeks later, the aorta with coronary of these mice were stained with hematoxylin–eosin.

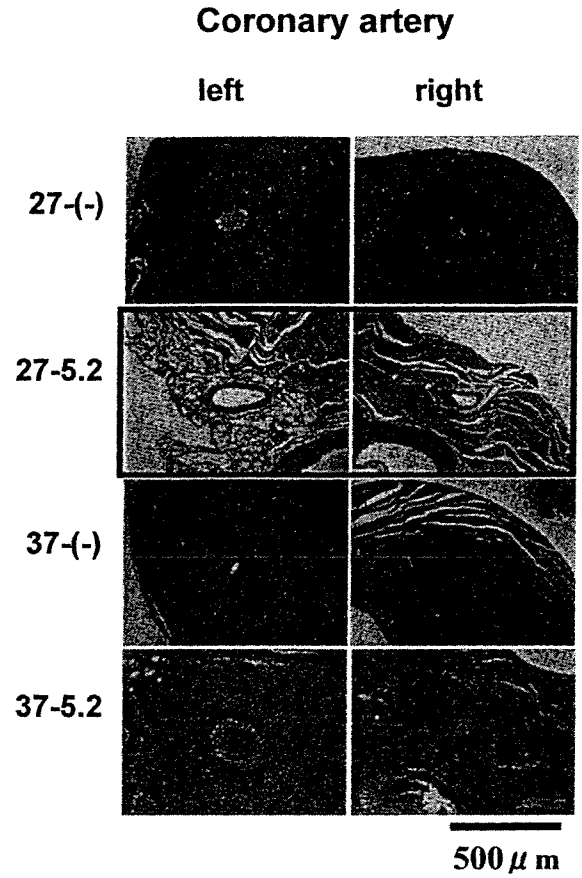

Fig. 8. Comparison of Histology of Coronary Artery in DBA/2 Mice Administered Native and pH-Controlled CAWS

CAWS 27-(–), CAWS 27-5.2, CAWS 37-(–), CAWS 37-5.2 (4 mg/mouse) were administered i.p. to DBA/2 mice for five consecutive days. Five weeks later, the artery with coronary of these mice were stained with hematoxylin–eosin.

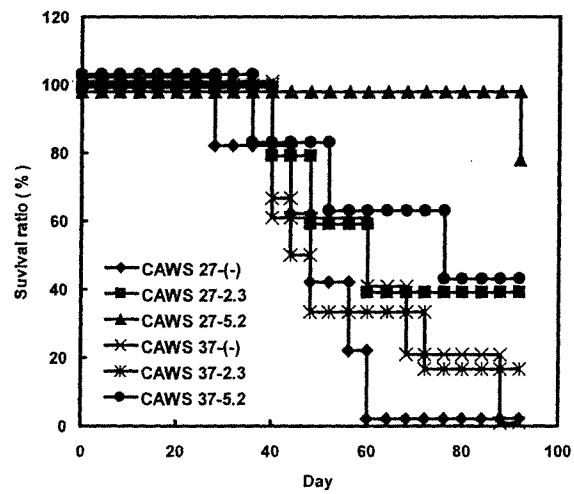

Fig. 9. Survival Time of CAWS-Administered Mice

CAWS 27s and CAWS 37s (4 mg/mouse) was administered i.p. to DBA/2 mice for five consecutive days in the 1st week. Survival was observed for 12 weeks.

CAWS 27-(–) was at least 20 times higher than that of CAWS 27-5.2. From these findings, CAWS with beta-1,2-linked mannooligosaccharides showed significantly weaker inflammatory reaction in this experimental model.

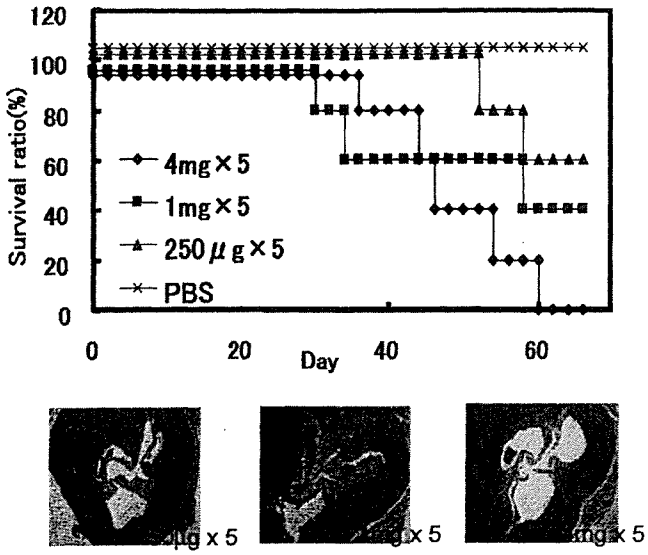

Fig. 10. Dose Response of Survival Time of CAWS-Administered Mice

CAWS 27-(–) (0.25, 1, or 4 mg/mouse) was administered i.p. to DBA/2 mice for five consecutive days in the 1st week. Survival was observed for 9 weeks. Hematoxylin–eosin stain of the aorta with coronary were also shown.

DISCUSSION

Candida albicans is a clinically important fungus and is known to cause disseminated candidiasis and candidemia in immunocompromised hosts. Patients with deep mycoses, such as that induced by *C. albicans* and *A. fumigatus*, have been demonstrated to release β-glucans into the blood. However, these are present in extremely small amounts, and the overall structure of the factor G activating substance present in the blood is unknown.[26] The factor G activating substance has the potential to exhibit various biological activities, but the details of this are also unknown. In order to clarify these matters, we first cultured *C. albicans* in a completely synthetic medium in order to obtain water-soluble limulus factor G activating substance that is released from the cells, and obtained a water-soluble polysaccharide fraction released into the culture supernatant (CAWS), which is thought to be similar to the β-1,3-D-glucan actually present in patient blood.[8] Murata *et al.* conducted an analysis on children with KD and found that *C. albicans* extract (CADS) isolated from the stool specimens of the patients induced coronary angiitis in mice that resembled KD.[5,6] During the course of joint research, we found that administration of CAWS according to this protocol induced a similar coronary angiitis in mice.[8–10]

In the present study, the relationship between culture conditions of *Candida* and induction of some of the pathologic parameters, such as acute shock, arteritis, and complement activation, was examined, and the condition producing beta-1,2-linkage significantly reduced all three parameters measured in the present study. It is of note that in the standard culture medium, C-limiting medium, the pH was acidified during culture. Thus, in the present study we have prepared CAWS in significantly regulated conditions and we analyzed both activity and structure. We have confirmed that CAWS prepared under the condition of neutral at 27 °C culture significantly reduced activity and is strongly related to the presence of beta-1,2-mannosyl linkages. These facts clearly demonstrated that beta-1,2-linkages are negative regulators for pathologic parameters, such as acute shock, arteritis, and complement activation. At this time, the role of beta-1,2-linkages on the anaphylactoid reaction and arteritis induction could not be fully clarified. As shown in Table 3, pretreatment of mice with CAWS 27-5.2 induced tolerance in the CAWS-induced anaphylactoid reaction, but this was less than that observed with CAWS 27-(–) and CAWS 27-2.3. In addition, small numbers of beta-1,2-linkages are present in CAWS 27-(–), which is comparable arteritis to CAWS 27-2.3. These facts strongly suggest that beta-1,2-linkages cover the active site, the alpha mannan moiety, of CAWS. Beta-1,2-linkage itself might not show receptor-mediated, specific and negative regulatory reactions.

Acute anaphylactoid reaction is known to be induced by lipopolysaccharide from *E. coli* O9 (O9 LPS), which possesses the mannose homopolysaccharide as the O-antigen region.[25] Very recently, we compared immunotoxicological and immunochemical similarity between CAWS and O9 LPS.[24] CAWS strongly reacted with *Candida* serum factors, and the reactivity was found to be partially competed with O9 LPS. CAWS-induced anaphylactoid reaction was inhibited by pretreatment of mice with i.p. injection of CAWS. The lethality was found to be inhibited by i.v. injection of O9 LPS. *Vice versa*, O9 LPS-induced acute anaphylactoid reaction in muramyl-dipeptide primed mice was also inhibited by pretreatment of mice with CAWS. These results suggested that CAWS and O9 LPS from gram-negative bacteria share, at least in part, immunochemical and immunotoxicological activities.

Mannose binding lectin (MBL) is a key molecule for innate immune response.[27] Neth *et al.* analyzed the concentration of MBL in various inbred strains and found that all of the strains tested contained MBL.[28] The MBL-A and MBL-C levels in 10 laboratory mice strains were 4 to 12 μg/ml, and 16 to 118 μg/ml, respectively. Higher concentration of MBL was detected in patients of rheumatic heart disease.[29] Point mutation in MBL is also related to severe atherosclerosis.[30] In the present study, we have shown contribution of the complement lectin pathway for the initiation of CAWS-induced anaphylactoid reaction and arteritis. We did not measure concentration of each complement components, and concentration of each component in inbred strains might be related to the phenotype of anaphylactoid reaction and arteritis.

The anaphylatoxin receptor is a family of G-protein coupled receptors (G-PCR).[31] It is well known that signaling of G-PCR induced cross talk and cross desensitization.[32] Cross desensitization of C5a receptor was reported with receptors of fMLP, IL-8, LTB4 and so on. Exaggerated inflammatory phenotype of bleomycin-induced lung fibrosis was shown in C5 knockout mice. DBA/2 is a strain deficient in C5. Severity of arteritis might be related to cross desensitization and may follow anti-inflammatory action of C5a receptor mediated signaling.

In the series of studies, we have analyzed CAWS-induced arteritis from various points of view. The most striking result was the significant strain dependency of arteritis as well as acute anaphylactoid reaction. For example, C3H/HeN is the most sensitive strain for anaphylactoid reaction but arteritis is moderate. DBA/2 is completely resistant to anaphylactoid reaction but shows the most severe arteritis. CBA/J is the

most resistant strain for arteritis but induced anaphylactoid reaction (unpublished results). B6 is sensitive to both anaphylactoid reaction and arteritis. These facts strongly suggest that the genes responsible for anaphylactoid reaction and arteritis would be at least in part different, and thus regulated by multiple genetic factors. However, from the point of early signaling events, activation of the lectin pathway of the complement by alpha-mannan moiety of CAWS might be key for both of the activities. Several reports indicated that *Candida albicans* could bind to MBL.[27,28]

We have shown that CAWS-induced arteritis and anaphylactoid reaction is dependent on strains of mice. In the present study, we demonstrated the essential structure to induce arteritis and anaphylactoid reaction. Strain specificity of both reactions was independent. We also analyzed the kinetics of arteritis induction and determined that it is separated into at least three phases, *i.e.*, early, middle, and late.[10] In the early phase, a variety of biochemical events is induced. In the middle phase, remodeling of arteries is induced. In the late phase, arteritis and coronary arteritis stressed heart function, resulting in cardiomegaly. Undoubtedly, multiple genes are involved in arteritis and cardiomegaly. This model proved very useful for analyzing whole steps of cardiac diseases.

Acknowledgements This work was partly supported by a Grant-in-Aid for Scientific Research from the Ministry of Education, Culture, Sports, Science and Technology of Japan, and The Promotion and Mutual Aid Corporation for Private Schools, Japan. Also supported by Ministry of Health, Labour and Welfare in Japan a Grant on "Research on Regulatory Science of Pharmaceuticals and Medical Devices."

REFERENCES

1) Shoham S., Levitz S. M., *Br. J. Haematol.*, **129**, 569—582 (2005).
2) Murata H., Iijima H., Naoe S., Atobe T., Uchiyama T., Arakawa S., *Jpn. J. Exp. Med.*, **57**, 305—313 (1987).
3) Kawasaki T., Kosaki F., Okawa S., Shigematsu I., Yanagawa H., *Pediatrics*, **54**, 271—276 (1974).
4) Furusho K., Kamiya T., Nakano H., Kiyosawa N., Shinomiya K., Hayashidera T., Tamura T., Hirose O., Manabe Y., Yokoyama T., *Lancet*, **2**, 1055—1058 (1984).
5) Oharaseki T., Kameoka Y., Kura F., Persad A. S., Suzuki K., Naoe S., *Microbiol. Immunol.*, **49**, 181—189 (2005).
6) Takahashi K., Oharaseki T., Wakayama M., Yokouchi Y., Naoe S., Murata H., *Inflamm. Res.*, **53**, 72—77 (2004).
7) Kurihara K., Shingo Y., Miura N. N., Horie S., Usui Y., Adachi Y., Yadomae T., Ohno N., *Biol. Pharm. Bull.*, **26**, 233—240 (2003).
8) Ohno N., *Microbiol. Immunol.*, **47**, 479—490 (2003).
9) Nagi-Miura N., Shingo Y., Adachi Y., Ishida-Okawara A., Oharaseki T., Takahashi K., Naoe S., Suzuki K., Ohno N., *Immunopharmacol. Immunotoxicol.*, **26**, 527—543 (2004).
10) Nagi-Miura N., Harada T., Shinohara H., Kurihara K., Adachi Y., Ishida-Okawara A., Oharaseki T., Takahashi K., Naoe S., Suzuki K., Ohno N., *Atherosclerosis*, **186**, 310—320 (2006).
11) Poulain D., Jouault T., *Curr. Opin. Microbiol.*, **7**, 342—349 (2004).
12) Masuoka J., *Clin. Microbiol. Rev.*, **17**, 281—310 (2004).
13) Bates S., Hughes H. B., Munro C. A., Thomas W. P., Maccallum D. M., Bertram G., Atrih A., Ferguson M. A., Brown A. J., Odds F. C., Gow N. A., *J. Biol. Chem.*, **281**, 90—98 (2006).
14) Arroyo-Flores B. L., Calvo-Mendez C., Flores-Carreon A., Lopez-Romero E., *FEMS Immunol. Med. Microbiol.*, **45**, 429—434 (2005).
15) Rouabhia M., Schaller M., Corbucci C., Vecchiarelli A., Prill S. K., Giasson L., Ernst J. F., *Infect. Immun.*, **73**, 4571—4580 (2005).
16) Munro C. A., Bates S., Buurman E. T., Hughes H. B., Maccallum D. M., Bertram G., Atrih A., Ferguson M. A., Bain J. M., Brand A., Hamilton S., Westwater C., Thomson L. M., Brown A. J., Odds F. C., Gow N. A., *J. Biol. Chem.*, **280**, 1051—1060 (2005).
17) Suzuki A., Takata Y., Oshie A., Tezuka A., Shibata N., Kobayashi H., Okawa Y., Suzuki S., *FEBS Lett.*, **373**, 275—279 (1995).
18) Jones J. M., *Clin. Microbiol. Rev.*, **3**, 32—45 (1990).
19) Fukazawa Y., Shinoda T., Tsuchiya T., *J. Bacteriol.*, **95**, 754—763 (1968).
20) Kobayashi H., Takahashi S., Shibata N., Miyauchi M., Ishida M., Sato J., Maeda K., Suzuki S., *Infect. Immun.*, **62**, 968—973 (1994).
21) Okawa Y., Goto K., Nemoto S., Akashi M., Sugawara C., Hanzawa M., Kawamata M., Takahata T., Shibata N., Kobayashi H., Suzuki S., *Clin. Diagn Lab. Immunol.*, **3**, 331—336 (1996).
22) Shibata N., Ikuta K., Imai T., Satoh Y., Satoh R., Suzuki A., Kojima C., Kobayashi H., Hisamichi K., Suzuki S., *J. Biol. Chem.*, **270** 1113—1122 (1995).
23) Okawa Y., Oikawa S., Suzuki S., *Biol. Pharm. Bull.*, **29**, 388—391 (2006).
24) Tada R., Nagi-Miura N., Adachi Y., Ohno N., *Biol. Pharm. Bull.*, **29**, 240—246 (2006).
25) Zhao L., Ohtaki Y., Yamaguchi K., Matsushita M., Fujita T., Yokochi T., Takada H., Endo Y., *Blood*, **100**, 3233—3239 (2002).
26) Miyazaki T., Kohno S., Mitsutake K., Maesaki S., Tanaka K., Ishikawa N., Hara K., *J. Clin. Microbiol.*, **33**, 3115—3118 (1995).
27) Ip W. K., Lau Y. L., *J. Infect. Dis.*, **190**, 632—640 (2004).
28) Neth O., Jack D. L., Dodds A. W., Holzel H., Klein N. J., Turner M. W., *Infect. Immun.*, **68**, 688—693 (2000).
29) Schafranski M. D., Stier A., Nisihara R., Messias-Reason I. J., *Clin. Exp. Immunol.*, **138**, 521—525 (2004).
30) Hegele R. A., Ban M. R., Anderson C. M., Spence J. D., *J. Investig. Med.*, **48**, 198—202 (2000).
31) Richardson R. M., Ali H., Tomhave E. D., Haribabu B., Snyderman R., *J. Biol. Chem.*, **270**, 27829—27833 (1995).
32) Addis-Lieser E., Kohl J., Chiaramonte M. G., *J. Immunol.*, **175**, 1894—1902 (2005).

THE JOURNAL OF BIOLOGICAL CHEMISTRY
Vol. 280, No. 1, Issue of January 7, pp. 94–103, 2005
Printed in U.S.A.

Phosphorylation of *Candida glabrata* ATP-binding Cassette Transporter Cdr1p Regulates Drug Efflux Activity and ATPase Stability*[S]

Received for publication, July 21, 2004, and in revised form, September 20, 2004
Published, JBC Papers in Press, October 21, 2004, DOI 10.1074/jbc.M408252200

Shun-ichi Wada‡§, Koichi Tanabe‡, Akiko Yamazaki‡, Masakazu Niimi‡¶‖, Yoshimasa Uehara‡¶, Kyoko Niimi‡‡, Erwin Lamping**‡‡, Richard D. Cannon**‡‡, and Brian C. Monk**‡‡**

*From the ‡Department of Bioactive Molecules, National Institute of Infectious Diseases, 1-23-1 Toyama, Shin-juku-ku, Tokyo 162-8640, Japan and the **Department of Oral Sciences, University of Otago, P. O. Box 647, Dunedin, New Zealand*

Fungal ATP-binding cassette transporter regulation was investigated using *Candida glabrata* Cdr1p and Pdh1p expressed in *Saccharomyces cerevisiae*. Rephosphorylation of Pdh1p and Cdr1p was protein kinase A inhibitor-sensitive but responded differentially to Tpk isoforms, stressors, and glucose concentration. Cdr1p Ser^{307}, which borders the nucleotide binding domain 1 ABC signature motif, and Ser^{484}, near the membrane, were dephosphorylated on glucose depletion and independently rephosphorylated during glucose exposure or under stress. The S484A enzyme retained half the wild type ATPase activity without affecting azole resistance, but the S307A enzyme was unstable to plasma membrane isolation. Studies of pump function suggested conformational interaction between Ser^{484} and Ser^{307}. An S307A/S484A double mutant, which failed to efflux the Cdr1p substrate rhodamine 6G, had a fluconazole susceptibility 4-fold greater than the Cdr1p expressing strain, twice that of the S307A mutant, but 64-fold less than the control null strain. Stable intragenic suppressors indicative of homodimer nucleotide binding domain 1-nucleotide binding domain 1 interactions partially restored rhodamine 6G pumping and increased fluconazole and rhodamine 6G resistance in the S307A/S484A mutant. Nucleotide binding domain 1 of Cdr1p is a sensor of important physiological stimuli.

Infections caused by *Candida* sp. are most frequently seen in immunocompromised individuals, including AIDS and leukemia patients. *Candida albicans* remains the leading cause of candidiasis, but the incidence of drug-resistant non-*albicans* *Candida* infections has become an increasingly significant clinical problem. *Candida glabrata* is among the most common of these pathogens (1), with many clinical isolates showing a 16- to 64-fold higher minimum inhibitory concentration (MIC)[1] of fluconazole (FLC) than *C. albicans* (2). Azole drugs such as FLC and itraconazole, which target lanosterol 14α-demethylase and block the synthesis of ergosterol, are well tolerated and widely used in the treatment of fungal disease. They are, however, fungistatic substrates of pleiotropic drug resistance (*PDR*) family ATP-binding cassette (ABC) transporters, and resistant fungi that overexpress these pumps are frequently isolated in the clinic (3). The *C. glabrata PDR* family ABC transporters Cdr1p and Pdh1p, which efflux azole agents and structurally unrelated compounds, are among the primary causes of the intrinsic resistance of *C. glabrata* to azole drugs (4–8). The two pumps have >70% amino acid sequence identity and transport a similar spectrum of substrates, but Cdr1p had greater drug efflux activity for most substrates. Structural information on fungal single subunit ABC transporters is rudimentary, and the molecular and regulatory features that determine their enzyme activity and substrate specificity are poorly understood. Such information is required for the rational design of pump inhibitors and antifungal drugs that are not pump substrates.

There are few reports of the effects of post-translational modification on the activity of fungal ABC transporters. Serine 420, a casein kinase-dependent phosphorylation site that determines *Saccharomyces cerevisiae* Pdr5p turnover (9), is the only experimentally proven fungal ABC transporter phosphorylation site. We have shown that the ATPase activity of Cdr1p and the drug efflux activity of Pdh1p are regulated by phosphorylation (7). Cdr1p cannot be phosphorylated at the position equivalent to Ser^{420}, whereas Pdh1p phosphorylation was regulated by protein kinase A (PKA) at one or more sites not homologous to Pdr5p Ser^{420}. More than one type of phosphorylation therefore occurs in fungal *PDR* family pumps.

This report describes the differential regulation of *C. glabrata* Cdr1p and Pdh1p expressed in *S. cerevisiae*. Immunological, physiological, and biochemical methods were applied to site-directed mutants in putative phosphorylation sites and to kinase-deletion mutants. PKA catalytic subunit isoforms differentially affected pump phosphorylation, and the effects of the phosphorylation of two putative novel sites in Cdr1p were determined. A phosphorylation site adjacent to the Cdr1p ABC signature motif

* This work was supported in part by a Grant-in-Aid from the Ministry of Education, Science, Sports and Culture of Japan. The costs of publication of this article were defrayed in part by the payment of page charges. This article must therefore be hereby marked "*advertisement*" in accordance with 18 U.S.C. Section 1734 solely to indicate this fact.

[S] The on-line version of this article (available at http://www.jbc.org) contains Supplemental "Materials and Methods," "Results," Figs. S1 and S2, and Refs. 1–6.

§ Supported by a Research Fellowship from the Japan Society for the Promotion of Science for Japanese Young Scientists. Current address: Dept. of Molecular Biology, The Scripps Research Institute, 10550 North Torey Pines Rd., La Jolla, CA 92037.

¶ Supported by the Health Science Research Grants for Research on Emerging and Re-emerging Infectious Diseases, Ministry of Health, Labor and Welfare of Japan.

‖ To whom correspondence should be addressed. Tel.: 81-3-5285-1111; Fax: 81-3-5285-1272; E-mail: niimi@nih.go.jp.

‡‡ Supported by the Japan Health Sciences Foundation and the Health Research Council of New Zealand.

[1] The abbreviations used are: MIC, minimum inhibitory concentration; FLC, fluconazole; PDR, pleiotropic drug resistance; ABC, ATP-binding cassette; PKA, protein kinase A; NBD, nucleotide binding domain; CSM, complete synthetic medium; Rh6G, rhodamine 6G; p-PKAs, phospho-(Ser/Thr) PKA substrate; p-Akts, phospho-Akt substrate; p-Thr, phospho-Threonine; BIM, bisindolylmaleimide I.

in nucleotide binding domain 1 (NBD1) affected the extent of multidrug efflux and the *in vitro* stability of ATPase activity while mutation of another cytoplasmic site nearer the membrane diminished transport at low glucose concentrations. Mutation in both sites eliminated the pumping activity of Cdr1p, whereas intragenic suppressors obtained by exposing the double mutant to FLC partially restored pump function. The Cdr1p NBD1 is a functional sensor of cell physiology and stress that may regulate interactions between homodimers.

EXPERIMENTAL PROCEDURES

Yeast Strains and Growth Media—Growth and selection media, and the methods used to prepare and mutate *S. cerevisiae* strains expressing Pdh1p and Cdr1p, are described in the Supplemental Data section.

Drug Susceptibility Assays—Agar diffusion assays on YPD (Qbiogene, Irvine, CA) agar plates, microplate MIC assays in HEPES and MES-buffered CSM (Qbiogene, Inc.) were performed, and the drugs and chemical compounds used were obtained as previously described (7).

Analysis of Pump Protein Phosphorylation—Glucose-starved yeast were obtained by incubation in CSM minus glucose for 3.5 h, and crude plasma membrane fractions were prepared as previously described (7) using GTED-20 buffer (10 mM Tris-HCl, pH 7.0, 0.5 mM EDTA, and 20% (v/v) glycerol) instead of the previous homogenization buffer. The membrane fractions were analyzed by SDS-PAGE and immunoblotting as previously described (7) using 1/2000 dilutions of anti-phospho (serine/threonine) protein kinase A substrate antibody, anti-phospho-(serine/threonine) Akt substrate antibody, and anti-phospho threonine antibody from Cell Signaling Technology (Beverly, MA), together with anti-rabbit IgG conjugated with horseradish peroxidase secondary antibody (Amersham Biosciences).

ATPase Assay—Purified plasma membrane fractions were prepared from cells grown in YPD to early stationary phase ($A_{600\ nm}$ = 7.0–9.0) and oligomycin-sensitive ATPase activities of samples were measured as previously described (7).

Fluorometric Assay of Rhodamine 6G Efflux—Log phase ($A_{600\ nm}$ = 1.5) cells grown in CSM-URA (Qbiogene, Inc., Irvine, CA) medium were stored overnight on ice. The cells were harvested by centrifugation, washed twice with distilled water, and then incubated in HEPES buffer (50 mM HEPES-NaOH, pH 7.0) containing 5 mM 2-deoxyglucose at 30 °C for 30 min to deplete intracellular energy levels. The cells were preloaded with 15 μM Rh6G for 30 min, washed twice, and resuspended in HEPES buffer at $A_{600\ nm}$ = 15 (1.5×10^8 cells ml^{-1}). Cell samples (50 μl) were incubated at 30 °C for 5 min and 50 μl of glucose at twice the final concentration added to start the reaction. After 8 min the cells in 80-μl samples were removed by passage through a Multi-well Filter plate (Acro Prep, Pall Corp.) placed on a Multiscreen resist vacuum manifold (Millipore), with a 96-well black flat-bottom microtiter collection plate (BMG Labtechnologies GmbH, Offenburg, Germany) underneath. The Rh6G content of the eluate, combined with two 80-μl washes with ice-cold HEPES buffer, was quantitated using a POLARstar OPTIMA (BMG Labtechnologies) fluorometer (excitation and emission wavelengths of 485 and 520 nm, respectively) with Fluostar OPTIMA software and a standard curve of Rh6G in the HEPES buffer.

RESULTS

Antibodies Recognizing Cdr1p or Pdh1p Phosphorylations—We have previously described the *S. cerevisiae* strains CDR1-AD and PDH1-AD, which contain a mutant Pdr1p transcriptional regulator and thus constitutively heterologously hyperexpress Cdr1p and Pdh1p, respectively, from the *PDR5* promoter (7, 10). Cdr1p and Pdh1p were hyperexpressed at comparable levels (~10% of plasma membrane protein) and were readily distinguished as heterologous plasma membrane proteins on Coomassie Blue-stained SDS-polyacrylamide gels due to the deletion of seven similar-sized, endogenous pump proteins. Each strain also showed the expected high level resistance to azole drugs (7). The pumps heterologously expressed in *S. cerevisiae* were therefore correctly folded and should be post-translationally regulated as in *C. glabrata*, because these two closely related yeasts have similar intracellular molecular machinery.

The phosphorylation of both Cdr1p and Pdh1p was detected by ^{32}P labeling, but the signals were too weak to support more

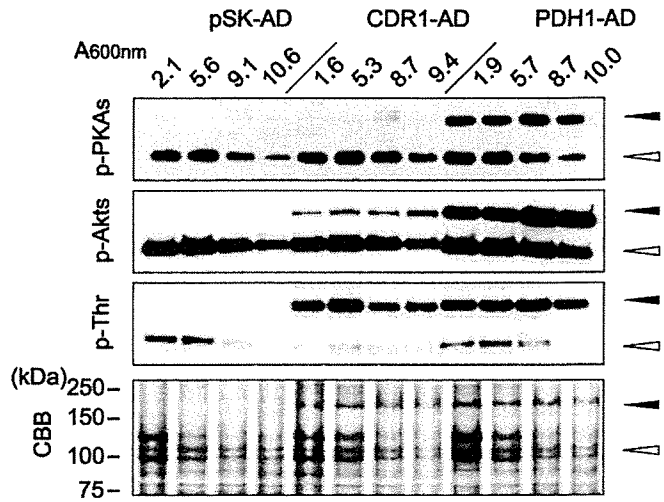

FIG. 1. **Phosphorylation of Cdr1p and Pdh1p.** The Cdr1p and Pdh1p-expressing yeast strains, CDR1-AD and PDH1-AD, and the empty vector integrated strain pSK-AD were cultured in YPD medium from initial $A_{600\ nm}$ = 0.005, 0.015, 0.05, and 0.15 values. After 14 h, the $A_{600\ nm}$ values of the cultures were measured (indicated at the *top*), and crude cell membrane fractions were prepared from the cells. Membrane samples containing 5 μg of protein were separated by SDS-PAGE, and the phosphorylation status of pump proteins was analyzed by immunoblotting using phospho-protein kinase A substrate (p-PKAs), phospho-(Ser/Thr), Akt substrate (p-Akts), and phospho-threonine (p-Thr) antibodies. The membrane fraction samples (15 μg of protein) were also separated by SDS-PAGE and stained with Coomassie Brilliant Blue R250 (*CBB*) to show relative protein expression levels. The 170-kDa Cdr1p and Pdh1p are indicated with a *black arrowhead*, and the control 100-kDa plasma membrane H^+-ATPase (Pma1p) band is indicated with a *white arrowhead*. Representative data from several experiments are shown.

detailed experiments. Neither Cdr1p nor Pdh1p reacted with phospho-protein kinase C substrates antibody or phospho-tyrosine antibodies (7). An anti-phospho-(Ser/Thr) PKA substrate (p-PKAs) antibody detected phosphorylation of Pdh1p but not Cdr1p or background ABC transporters in Western blots of plasma membrane preparations (Fig. 1).

Antibodies with different specificities detected novel phosphorylation sites in Cdr1p and Pdh1p. The anti-phospho-Akt substrate (p-Akts) and anti-phospho-threonine (p-Thr) antibodies recognized the phosphorylation of Cdr1p and Pdh1p expressed in all growth phases of YPD culture (Fig. 1, *black arrowheads*). Cdr1p expression in CDR1-AD decreased slightly in stationary phase (Fig. 1, *CBB staining*), whereas the p-Akts antibody recognition signal increased. Conversely, the p-Thr antibody gave a stronger signal in the log phase preparation. Cdr1p is therefore multiply phosphorylated at discrete p-Akts and p-Thr antibody recognition sites. Pdh1p phosphorylation in the PDH1-AD strain was readily detected by the p-PKAs, p-Akts, and p-Thr antibodies, with constant signals obtained throughout all growth phases of YPD culture. The recognition of the 100-kDa protein, which co-migrates with the constitutively expressed plasma membrane ATPase Pma1p (Fig. 1, *white arrowheads*) by the three antibodies provided an internal control for both the CDR1-AD and PDH1-AD preparations.

Glucose-sensitive Phosphorylation of Pdh1p and Cdr1p—We previously found that the Cdr1p and Pdh1p pumps were extensively dephosphorylated after a few hours of glucose starvation and immediately rephosphorylated when 2% glucose was added (7). The glucose concentration dependence of each rephosphorylation was therefore determined (Fig. 2*A*). Early stationary phase YPD cultures were glucose-starved for 3.5 h and then treated for 10 min with 10 μM, 1 mM, or 100 mM glucose. Rephosphorylation of Cdr1p was detected with p-Akts and p-Thr antibodies, but only after exposure to 100 mM glucose.

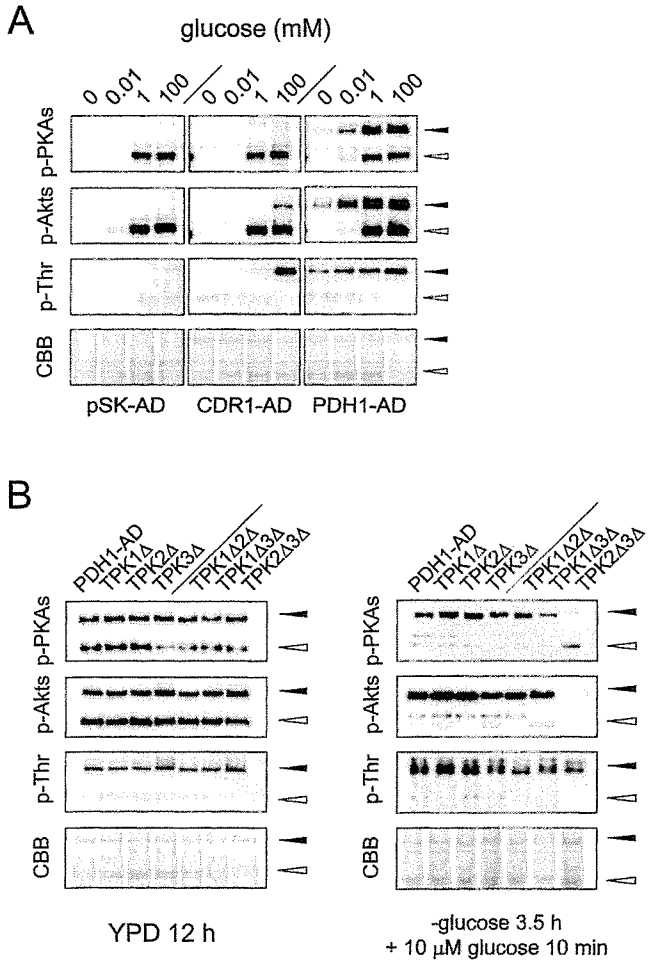

FIG. 2. **Glucose-sensitive phosphorylation of Pdh1p.** *A*, early stationary phase pSK-AD, CDR1-AD, or PDH1-AD cells from YPD culture were washed with distilled water and glucose-starved in CSM minus glucose (*CSM-Gluc*) for 3.5 h. Distilled water (0), 10 μM, 1 mM, or 100 mM glucose was then added to samples of cells for 10 min, and crude membrane fractions were prepared. Membrane fractions of 5 μg and 15 μg of protein were analyzed by immunoblotting and Coomassie Brilliant Blue R250 (*CBB*) staining, respectively, as described in Fig. 1. *Arrowheads* indicate Cdr1p and Pdh1p (*black*) and Pma1p (*white*). Representative data from several experiments are shown. *B*, PDH1-AD and its derivative single *TPK* gene-defective strains, PDH1-TPK1Δ (*TPK1* deleted), PDH1-TPK2Δ, and PDH1-TPK3Δ, and the double *TPK* gene-defective strains, PDH1-TPK1Δ2Δ (*TPK1* and *TPK2* deleted), PDH1-TPK1Δ3Δ, and PDH1-TPK2Δ3Δ were grown in YPD to early stationary phase (*YPD 12 h*), some cells were then glucose-starved for 3.5 h and treated with 10 μM glucose for 10 min. The phosphorylation and rephosphorylation pattern and expression level of Pdh1p in each strain was detected as described in Fig. 1. Representative data from several independently isolated clones of each strain are shown.

Pdh1p remained partially phosphorylated after glucose starvation, but all three antibodies detected glucose-dependent rephosphorylation at a glucose concentration (10 μM) that failed to induce Pma1p phosphorylation. The different phosphorylation patterns detected with each antibody indicated that Pdh1p was also rephosphorylated at multiple sites. The >100-fold differential in the glucose-dependence of Cdr1p and Pdh1p phosphorylation suggested that the two pumps were modified by different kinases/phosphatases or had sites with different susceptibilities to phosphorylation.

Pdh1p phosphorylation at p-PKAs sites is inhibited by PKA inhibitors (7). A panel of PKA catalytic subunit (Tpk) single and double deletion mutants was used to identify the *TPK* gene product that regulated Pdh1p phosphorylation in PDH1-AD. The three genes (*TPK1*, *-2*, and *-3*) encoding these PKA catalytic subunit isoforms can be deleted without lethality, either singly or up to two at a time (11). In YPD culture, identical Pdh1p phosphorylation signals were observed, even in the double deletion mutants PDH1-TPK1Δ2Δ, -TPK1Δ3Δ, and -TPK2Δ3Δ (Fig. 2*B*). In contrast, rephosphorylation at the PKA and Akt sites was not induced by 10 μM glucose in PDH1-TPK2Δ3Δ, and PKA site rephosphorylation was dramatically decreased in PDH1-TPK1Δ3Δ (Fig. 2*B*). Thus Tpk3p was the main contributor to glucose-dependent rephosphorylation of Pdh1p PKA and Akts sites at low glucose concentrations, and only Tpk2p could augment this process.

Stress Sensitivity of Cdr1p and Pdh1p Phosphorylation—The glucose-dependent differences in Cdr1p and Pdh1p rephosphorylation patterns suggested that the two pumps might be phosphorylated in discrete physiological contexts. This hypothesis was initially tested for Cdr1p rephosphorylation in glucose-starved CDR1-AD by adding 1 mM glucose together with a stressor for 10 min (Fig. 3*A*). The 1 mM glucose supplied sufficient ATP as kinase substrate, because the Pma1p band was strongly phosphorylated even in the absence of Akt site phosphorylation of Cdr1p (Figs. 2*A* and 3*A*). The pump substrate FLC (45 μg/ml) did not affect rephosphorylation (data not shown), but oxidative stress (2 mM H_2O_2), osmotic stress (500 mM NaCl), and heat shock (42 °C) for 10 min induced p-Akt site phosphorylation, albeit to a lesser extent than 100 mM glucose (Fig. 3*A*). Stress-dependent rephosphorylation was not detected with the p-Thr antibody. Pdh1p in PDH1-AD was highly phosphorylated in 1 mM glucose, and stress treatments caused no additional phosphorylation. In contrast, stress with 2 mM H_2O_2 alone decreased Pdh1p phosphorylation and gave no rephosphorylation of Cdr1p. However, Cdr1p phosphorylation was not affected when the yeast in YPD culture were stressed (H_2O_2, NaCl, or 42 °C) for 10 min (data not shown). Under these conditions, the effects of multiple kinases and phosphatases may have been complex and/or compensatory.

Rephosphorylation of Cdr1p Akt sites was inhibited by the PKA inhibitors H-89 and amide 14–22 but not by the H-89 homologue H-8, which has a K_i for PKA 30-fold higher than H-89 (12), or the protein kinase C inhibitor bisindolylmaleimide I (BIM) (Fig. 3*B*). A panel of *TPK* single or double deletion mutants constructed in CDR1-AD was tested for the effects of NaCl- and glucose-dependent rephosphorylation of Cdr1p (Fig. 3*C*). Apart from CDR1-TPK1Δ2Δ and CDR1-TPK2Δ3Δ, which reduced Cdr1p rephosphorylation by about 50% during both treatments, p-Akts site re-phosphorylation was unaffected. Thus Tpk2p and to a lesser extent Tpk1p and Tpk3p may play a role with other kinases susceptible to PKA inhibitors in the rephosphorylation of Cdr1p Akts sites.

Identification of Putative Phosphorylation Sites in Cdr1p—Modest rephosphorylation signals suggested the presence of few p-Akts sites in Cdr1p. The p-Akts antibody recognizes phosphorylated Ser or Thr in the $^{-5}$(K/R)X^{-3}(K/R)XX^{0}(S/T) motif and cross-reacts with the phosphorylated $^{-3}$(K/R)$^{-2}$(K/R)X^{0}(S/T) motif (manufacturer's information). The full size, single subunit, ABC transporter Cdr1p comprises two nucleotide binding domains (NBD1 and NBD2) that each contain the Walker A, Walker B, and ABC signature motifs, alternating with two pairs of six transmembrane segments, as illustrated in Fig. 4*A*. We constructed the yeast strains CDR1-M1 to CDR1-M9, which expressed equivalent amounts of Cdr1p (Fig. 4*B*), and each contained a point mutation (S/T → A) at each one of the nine putative p-Akts recognition sites. Of these sites, only M2, M4, and M7 may be recognized by the phospho-PKA substrates antibody (phosphorylated Ser or Thr in R*XX*(S/T)). Unlike the essentially normal phosphorylation of Cdr1p p-Akts sites in the CDR1-M3-CDR1-M9 mutants in 12-h YPD (early

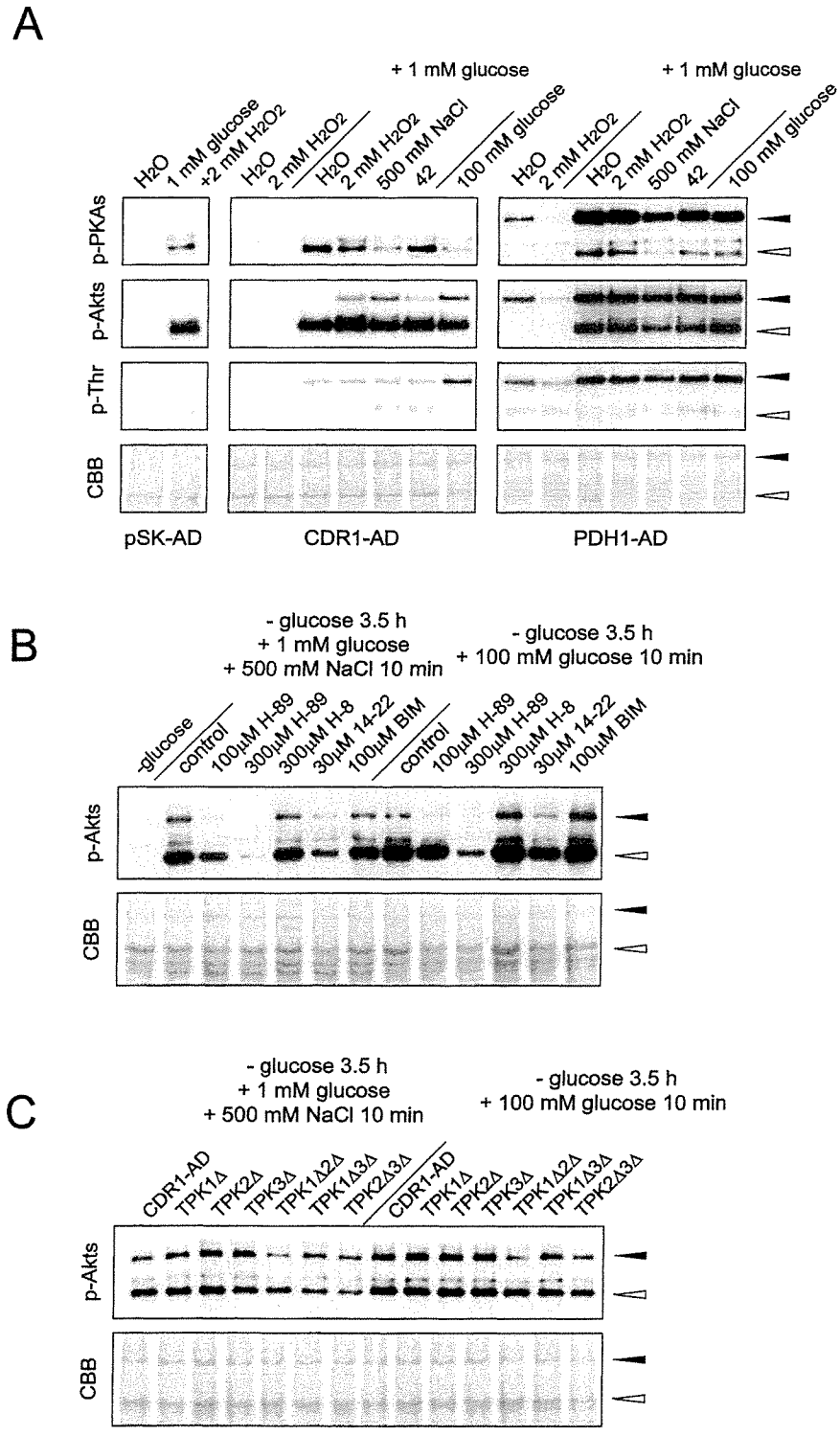

FIG. 3. **Stress- and kinase-dependent phosphorylation of Cdr1p.** *A*, glucose-starved pSK-AD, CDR1-AD, or PDH1-AD cells were stressed or treated with 100 mM glucose for 10 min as indicated in the *top panel*. Stress experiments that included 1 mM glucose are indicated. Phosphorylation patterns and expression levels of pump proteins were determined as in the previous figures. *B*, glucose-starved CDR1-AD (*−glucose*) cells were treated with protein kinase inhibitors H-89, H-8, 14–22 amide (14–22), bisindolylmaleimide I (*BIM*), or a solvent control (1% Me_2SO plus 1% water). After 10 min, 500 mM NaCl plus 1 mM glucose, or 100 mM glucose was added, the cells cultured for 10 min, and crude membrane fractions were prepared for analysis. *C*, single and double *TPK* gene deletion mutants were constructed from CDR1-AD as described for PDH1-AD (Fig. 2). Glucose-starved CDR1-AD and the derivative *TPK* deletion mutants were treated with 500 mM NaCl, and 1 mM glucose, or 100 mM glucose for 10 min. The phosphorylation patterns and protein expression levels of the crude membrane fractions were analyzed.

stationary phase) cultures, Cdr1p phosphorylation was eliminated in CDR1-M1 and >90% inhibited in CDR1-M2 (Fig. 4*B*). Rephosphorylation of Cdr1p-M1 and Cdr1p-M2 was not detected in response to stressors plus 1 mM glucose (Fig. 4, *C* and *D*), and 100 mM glucose gave rephosphorylation to about 50% of the control level in each mutant (Fig. 4*D*). These results suggested that Ser^{307} and Ser^{484} are the dominant Akts sites in Cdr1p. This hypothesis was confirmed by finding, in the S307A/S484A double mutant strain CDR1-M1,2, that 100 mM glucose gave no Cdr1p p-Akts site rephosphorylation (Fig. 4*E*). Thus, the phosphorylation of M1 and M2 sites responded comparably to 12-h YPD culture (low glucose) and stressors, whereas glucose-induced rephosphorylation of the two sites occurred independently. Interestingly, the S307A mutation of the M1 site mutation reduced Thr phosphorylation by one-third in 12-h YPD cultures (Fig. 4*B*), and the S509A mutation at the membrane-associated M3 site similarly affected Akts site rephosphorylation of Cdr1p in 100 mM glucose (Fig. 4*E*).

Rhodamine 6G Efflux from Pdh1p, Cdr1p, and Point Mutant Yeast—The effect of the M1 and M2 mutations on energy-dependent drug efflux by Cdr1p was quantitated by comparably pre-loading CDR1-AD, CDR1-M1, CDR1-M2, CDR1-M1,2 and AD1–8u$^-$ cells with the pump substrate rhodamine 6G (Rh6G) after 2-deoxyglucose treatment and then stimulating efflux by

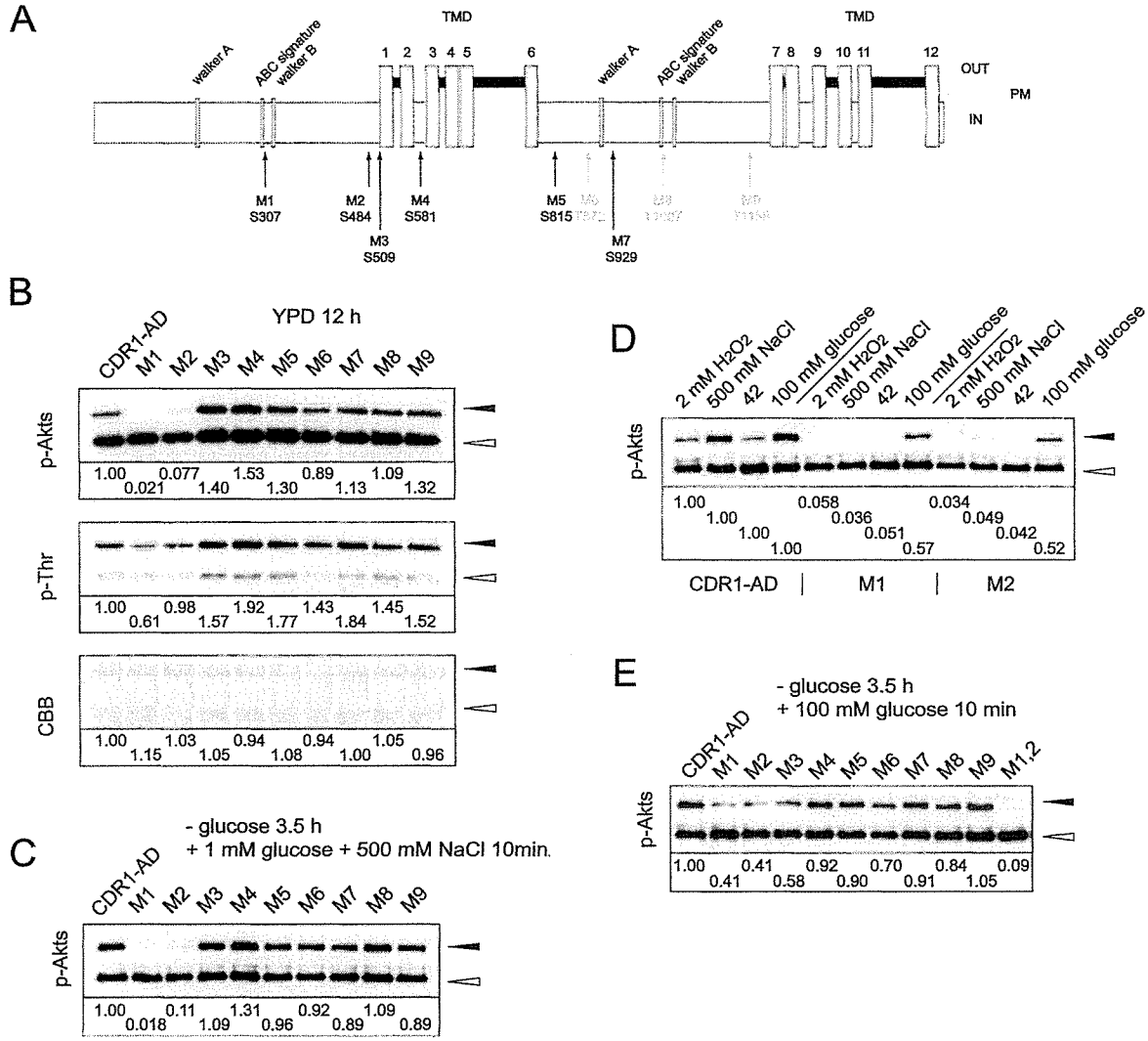

FIG. 4. **Phosphorylation sites of Cdr1p detected by the phospho-(Ser/Thr) Akt substrate antibody.** *A*, the nine putative phospho-Akt substrate antibody recognition sites (p-Akts sites) $^{-5}$(K/R)*X*$^{-3}$(K/R)*XX* ^{0}(S/T) or $^{-3}$(K/R)$^{-2}$(K/R)*X*^{0}(S/T) of Cdr1p are shown (M1–M9), with Ser in *black* and Thr in *gray*. The conserved motifs of the nucleotide binding cassette, Walker A, B, and ABC signature, and twelve trans-membrane domains (*TMD*) are depicted with *gray bars*, whereas regions external to the plasma membrane (*PM*) are shown in *black*. CDR1-M1 through CDR1-M9 yeast strains, whose Ser or Thr residues were replaced by Ala at each M1–M9 site, were constructed. *B*, the phosphorylation patterns and expression levels of Cdr1p in crude membrane fractions from CDR1-AD and the point mutated derivatives CDR1-M1 through CDR1-M9 grown to early stationary phase in YPD medium were measured as described in previous figures. The ratios of intensities relative to CDR1-AD (1.0), given at the *bottom of each panel*, were measured using Scion Image. *C*, CDR1-AD and its derivative mutant strains were glucose-starved for 3.5 h and treated with 1 mM glucose and 500 mM NaCl for 10 min. The phosphorylation status of the Akt sites in each mutant Cdr1p was analyzed as above. *D*, glucose-starved CDR1-AD, -M1, and -M2 yeasts were treated with stressors and 1 mM glucose, or 100 mM glucose for 10 min as indicated in the *top panel*. The patterns of Cdr1p phosphorylation were analyzed as above. The relative band intensities are shown for each stress condition. *E*, CDR1-AD, the point mutants CDR1-M1 through CDR1-M9, and CDR1-M1,2 were glucose-starved for 3.5 h and then treated with 100 mM glucose for 10 min. The phosphorylation of Cdr1p was analyzed as above. In *B–E*, Cdr1p and the equivalent bands from the point mutant derivatives are indicated with the *black arrowhead*, whereas the Pma1p band is indicated with the *white arrowhead*. Representative data, from multiple experiments using several independently isolated clones of each strain, are shown.

adding glucose (Fig. 5). Fluorometric measurements showed that the CDR1-M2 strain (half-maximal rate of Rh6G pumping, 2.5 mM glucose; maximal pumping rate, 5–10 mM glucose) pumped Rh6G at rates up to 80% of the CDR1-AD strain (half-maximal rate of Rh6G pumping, 1 mM glucose; maximal rate, 5–10 mM glucose). In contrast, the CDR1-M1 strain required at least 5 mM glucose for a significant rate of Rh6G efflux and reached a maximal rate at 20 mM glucose, which was only 30% that of the CDR1-AD strain. The CDR1-M1,2 strain showed no glucose-dependent Rh6G efflux, even at 100 mM glucose. All strains that effluxed Rh6G showed a 30% decrease in the pumping rate at glucose concentrations between 20 and 100 mM glucose.

The pumping activities of Cdr1p and its point mutants were confirmed by flow cytometric measurement of cellular Rh6G content, which monitors combined dye uptake and efflux (see Supplemental Data, Fig. S1). These data also showed that strain CDR1-M1,2 did not efflux Rh6G even in the presence of 100 mM glucose and that phosphorylation of the Cdr1p-M1 site may be required for Rh6G efflux at low glucose concentrations.

Lability of ATPase Activity in CDR1-M1—The Cdr1p drug efflux pumps were functional in CDR1-M1, CDR1-M2, and CDR1-M8 cells and therefore expected to retain significant ATPase activity on cell fractionation. Plasma membrane fractions from these strains contained equivalent amounts of Cdr1p proteins, CDR1-M8 had a normal oligomycin-sensitive ATPase activity with a broad pH profile, but CDR1-M2 showed a decrease of ~50% in the ATPase activity compared with CDR1-AD (Fig. 6). CDR1-M8 was chosen as a control, because the T1007A mutation borders the NBD2 ABC signature motif

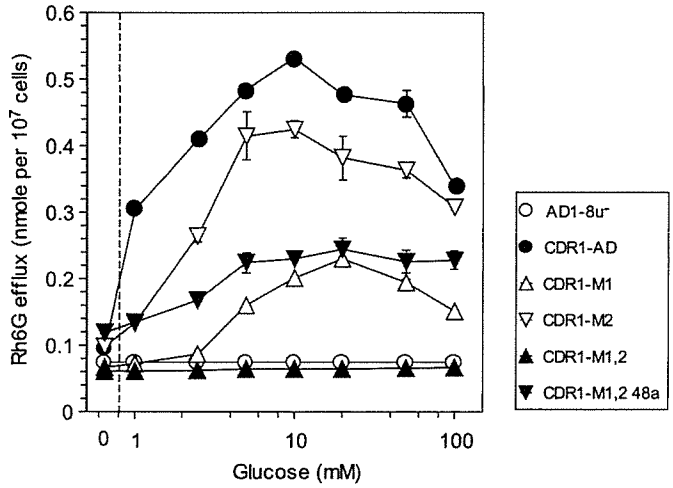

FIG. 5. **Glucose dependence of Rh6G efflux by CDR1-AD derivatives.** The efflux of Rh6G (mean ± S.D., $n = 3$) by glucose-starved cells preloaded in the presence of 2-deoxyglucose was measured by fluorometry as described under "Experimental Procedures." Strain M1,2 48a is the CDR1-M1,2 glucose-grown revertant 48a (D32H) described in Table II.

residue and aligns with Ser^{307} of NBD1. The membranes from CDR1-M1, however, lacked detectable oligomycin-sensitive ATPase activity. The M1 site may therefore be critical for the *in vitro* ATPase activity. Experiments that included ATP during membrane isolation allowed the recovery of small amounts (10%) of vanadate and oligomycin-sensitive ATPase activity compared with the control strain (see Supplemental Data Table SIII). A statistically significant proportion of this activity ($p < 0.01$) can be attributed to S307A Cdr1p that survived membrane isolation due to the protective ATP.

Drug Susceptibilities of CDR1-AD and PDH1-AD Derivative Yeasts—The MIC_{80} values for antifungal agents were determined for PDH1-AD and CDR1-AD derivative strains to assess whether the phosphorylation of Cdr1p and Pdh1p affected drug efflux activity (Table I). As expected, the Pdh1p- and Cdr1p-expressing strains were more resistant to azole agents than the control pSK-AD strain but were equally susceptible to flucytosine and amphotericin B, which are not pump substrates. The flucytosine and amphotericin B susceptibilities for all the strains were within two dilutions of the values for pSK-AD. Among the CDR1-AD derivatives, only CDR1-M1 and CDR1-M1,2 consistently showed lower FLC susceptibilities than CDR1-AD, giving values that were reproducibly 2-fold and 4-fold lower, respectively. The *TPK2* deletion mutants CDR1-TPK2Δ, -TPK1Δ2Δ, and -TPK2Δ3Δ gave detectably greater azole resistance than the control Cdr1p-expressing strain. Repeated testing of Cdr1p phosphorylation in *TPK2* deletion mutants found no relationship between the phosphorylation status of Cdr1p and the apparent azole resistance (data not shown). In contrast, the azole resistance of PDH1-AD *TPK* mutants was unchanged compared with the control parental strain. A SCH9 kinase deletion mutant and a HOG1 kinase deletion mutant of CDR1-AD both gave slightly increased resistance to azole agents. The former showed increased phosphorylation of Cdr1p Akts sites, and the latter had an unchanged phosphorylation pattern compared with the parental strain (data not shown).

Agar diffusion tests of susceptibilities of CDR1-AD, CDR1-M1, CDR1-M2, and CDR1-M1,2 to structurally unrelated xenobiotics extended the data on antifungal susceptibility reported in Table I and suggested that the M1 and M2 sites are synergistic effectors of Cdr1p drug efflux activity (see Supplemental Data Fig. S2). Of the 17 compounds to which CDR1-AD was strongly resistant (7), CDR1-M1 showed increased susceptibility to eight compounds, whereas CDR1-M1,2 had even greater susceptibility to these and two other compounds. In contrast, the susceptibilities of CDR1-AD and CDR1-M2 were indistinguishable.

The relatively high FLC MIC value for the CDR1-M1 strain (Table I) can be explained by partially functional mutant Cdr1p operating at glucose concentrations >5 mM. The lack of Rh6G pumping by CDR1-M1,2 (Fig. 5), however, seemed inconsistent with its relatively high MIC for FLC and other azoles (Table I), although this was less pronounced in disk diffusion assays. CDR1-M1,2 was also more resistant to FLC than either PDH1-AD or the AD1–8u⁻ host strain (Table I). Even though identical FLC and Rh6G susceptibilities were observed with three separately isolated clones for each construct under study, we excluded the possibility that secondary mutations in the genetic background of the strains might affect susceptibilities to azoles. *CgCDR1-URA3* DNA, obtained by PCR of genomic DNA of CDR1-AD, CDR1-M1, CDR1-M2, and CDR1-M1,2, was used to transform the hypersensitive AD1–8u⁻ strain. All tested Ura^+ transformants that grew normally on 5 μg/ml FLC (to ensure the incorporation of the *CDR1* gene) showed FLC and Rh6G susceptibilities identical to those for the strains providing the transforming DNA (Table II). The drug resistance of each donor strain was thus conferred by the expression of Cdr1p and not an extragenic determinant. The unexpectedly high FLC and Rh6G liquid MIC_{80} values for CDR1-M1,2 were therefore due to Cdr1-M1,2p overexpression. It was possible, however, that suppressor mutations were selected during growth in liquid MIC assays.

Progeny that survived FLC exposure during MIC determinations in buffered FLC-containing CSM-URA medium, using either glucose or the non-fermentable substrate glycerol as energy source, were isolated. Sequencing of several independent isolates showed that the S307A and S484A mutations were maintained in these progeny independent of the energy source. In addition, three independently isolated intragenic suppressor mutations were obtained that did not change the Ser^{307} and Ser^{484} background: a ΔA349 mutation after growth on glycerol and D32H and V353L mutations after growth on glucose. In contrast to the inactive parental CDR1-M1,2 strain, all three suppressor strains showed glucose-dependent Rh6G pumping comparable to the CDR1-M1 mutant. An Rh6G efflux experiment conducted with the representative suppressor strain CDR1-M1,2 48a is shown in Fig. 5. The *CgCDR1-URA3* cassette was obtained by PCR of genomic DNA from each of the three suppressor strains and used to transform strain AD1–8u⁻. The Ura^+ transformants that also grew on 5 μg/ml FLC showed FLC and Rh6G resistance comparable to the CDR1-M1 strain (Table II). The suppressor mutation phenotypes therefore result from intragenic modification of Cdr1p in CDR1-M1,2. The selection of the suppressor mutants occurred at a low frequency (suppressor strains were detectable in <10% of MIC determinations). This frequency was not high enough to compromise the MICs for azole drugs and other xenobiotic substrates of CDR1-M1,2.

DISCUSSION

Phosphorylation of ABC Transporters—Phosphorylation mediated by PKA and PKC affects the function of numerous human ABC transporters, including ABCA1, MDR1, and CFTR (13–15). We previously demonstrated that PKA-dependent phosphorylation of *C. glabrata* Pdh1p was important for drug efflux and Cdr1p ATPase specific activity was glucose-dependent and possibly regulated by phosphorylation (7). *C. glabrata* Cdr1p and Pdh1p have about 70% amino acid sequence identity with *S. cerevisiae* Pdr5p and thus belong to the *PDR* family, the

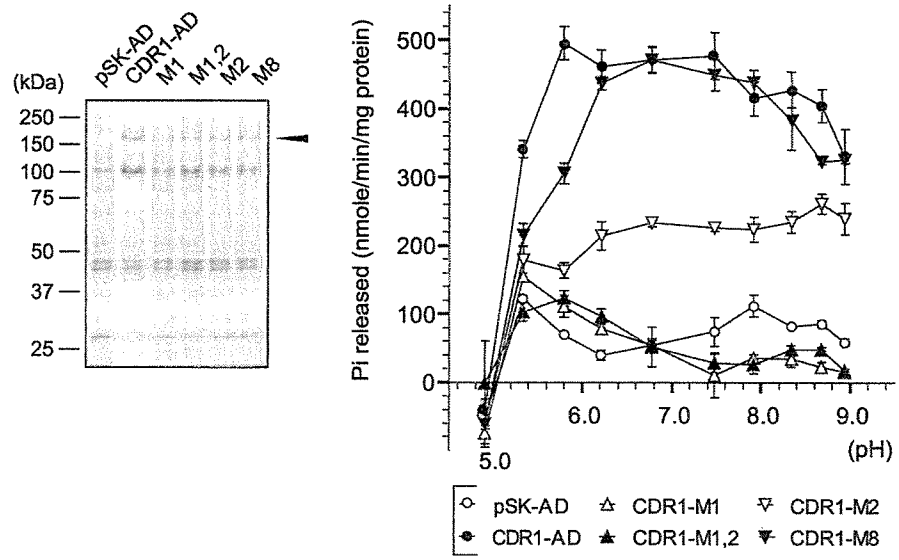

FIG. 6. **Loss of ATPase activity in mutated Cdr1p.** Plasma membrane fractions were prepared from pSK-AD, CDR1-AD, CDR1-M1, CDR1-M2, CDR1-M1,2, and CDR1-M8 yeast at early stationary phase of YPD culture. Oligomycin-sensitive ATPase activities of each fraction were measured at each pH indicated. Experiments were performed several times using the membrane fractions prepared from independently isolated clones of the yeast. Representative data for ATPase activities are shown on the *right* (mean ± S.E., $n = 3$), and the SDS-PAGE Coomassie Brilliant Blue R250 (*CBB*) staining patterns for 5 μg of protein of each membrane fraction used in the experiment are shown on the *left*. The *arrowhead* indicates Cdr1p.

TABLE I
Antifungal susceptibilities of CDR1-AD and PDH1-AD derivative strains

Strain	MIC_{80}[a]				
	Fluconazole	Miconazole	Ketoconazole	Flucytosine	Amphotericin B
			μg/ml		
pSK-AD	0.5	0.016	0.063	0.5	0.25
CDR1-AD	128	2	4	2	0.5
CDR1-M1	64	2	4	1	0.5
CDR1-M2	128	2	4	1	0.5
CDR1-M3	128	2	4	1	0.5
CDR1-M4	128	2	4	1	0.5
CDR1-M5	128	2	4	1	0.5
CDR1-M6	128	2	4	1	0.5
CDR1-M7	128	2	4	1	0.5
CDR1-M8	128	2	4	1	0.5
CDR1-M9	128	2	4	1	0.5
CDR1-M1,2	32	1	2	1	0.5
CDR1-TPK1Δ	128	2	4	2	0.5
CDR1-TPK2Δ	256	4	8	2	0.5
CDR1-TPK3Δ	128	2	4	2	0.5
CDR1-TPK1Δ2Δ	256	4	4	2	0.5
CDR1-TPK1Δ3Δ	128	2	4	2	1
CDR1-TPK2Δ3Δ	256	4	8	1	0.25
CDR1-SCH9Δ	256	4	8	0.25	0.25
CDR1-HOG1Δ	256	4	8	2	1
PDH1-AD	16	0.5	1	1	0.5
PDH1-TPK1Δ	16	0.5	1	1	0.5
PDH1-TPK2Δ	16	0.5	1	1	0.5
PDH1-TPK3Δ	16	0.5	1	1	1
PDH1-TPK1Δ2Δ	16	1	1	2	0.5
PDH1-TPK1Δ3Δ	16	0.5	1	2	1
PDH1-TPK2Δ3Δ	16	0.5	1	1	0.5

[a] MIC_{80} values (μg/ml) were the lowest concentration of drug that inhibited the growth yield by at least 80% compared with the growth yield for a non-drug control.

largest ABC transporter family in *S. cerevisiae* (16, 17). The *S. cerevisiae* drug efflux transporters Pdr5p, Snq2p, and Yor1p are all phosphorylated, and casein kinase I phosphorylation of Ser^{420} in Pdr5p is important for enzyme turnover (9), but the equivalent site is absent in Cdr1p. Phosphorylation of Thr^{613} and Ser^{623} in the D-box linking the two homologous halves of Ste6p has been implicated in enzyme turnover (18). The Cdr1p p-Akts antibody recognition sites at Ser^{307} and Ser^{484} are therefore distinct from the sites affecting Pdr5p and Ste6p turnover. The Ser^{307} and Ser^{484} sites appear physiologically important. They affect the glucose dependence of pump activity, and glucose-dependent Rh6G efflux was eliminated by the S307A/S484A double mutation. The expression of S307A, S484A, and the S307A/S484A double mutant Cdr1ps at levels comparable with the wild type protein implies that misfolding does not target the mutant proteins for early degradation. The PKA-dependent phosphorylation of human ABCA1 (13) provides a precedent for phosphorylation at Ser^{307}.

Kinases Responsible For the Phosphorylation of Pdh1p and of Cdr1p at M1 and M2 Sites—The glucose-dependent rephosphorylation of Pdh1p in starved cells was blocked by PKA inhibitors (7) and was primarily affected by Tpk3p and to a lesser extent by Tpk2p. Antibody recognition of phosphorylated PKA sites implies that these phosphorylations were direct. Of the nine putative phosphorylation sites tested in glucose-starved Cdr1p, only Ser^{307} and Ser^{484} strongly affected the rephosphorylation pattern. Unlike Pdh1p phosphorylation, neither site was recognized by the p-PKA substrates antibody after stress or at glucose concentrations 100-fold higher than those required for Pdh1p p-Akts site rephosphorylation. The blockage